Pathways in uremic cardiomyopathy – the intracellular orchestrator PGC-1α in cell culture and in a mouse model of uremia

*****

Intrazelluläre Vorgänge bei Urämischer Kardiomyopathie – die Rolle von PGC-1α in Zellkultur und im Mausmodell

Doctoral thesis for a medical doctoral degree

at the Graduate School of Life Sciences,

Julius-Maximilians-Universität Würzburg,

Section Biomedicine

submitted by

Tim Jonas Bergmann

from

Finschhafen, Papua New Guinea

Würzburg 2020

Submitted on:

11/17/2020

Members of the Thesis Committee:

Chairperson: Prof. Dr. rer. nat. Uwe Gbureck

Primary Supervisor: Prof. Dr. med. Christoph Wanner, Würzburg

Supervisor (Second): PD Dr. med. Christiane Drechsler, Würzburg

Supervisor (Third): Prof. Dr. med. Stefan Störk, Würzburg

Date of Public Defence:

07/11/2022

Date of Receipt of Certificates:

The doctoral candidate is an approbated physician.

FOR MY FAMILY

TABLE OF CONTENTS

1. INTRODUCTION 1

1.1 CHRONIC KIDNEY DISEASE: OVERVIEW 1
1.2 PATHOPHYSIOLOGICAL CHANGES IN CKD: UREMIC CARDIOMYOPATHY 6
1.3 UREA – JUST METABOLIC WASTE? 6
1.4 PGC-1A – ORCHESTRATOR OF MITOCHONDRIAL METABOLISM 7
1.5 OBJECTIVE OF RESEARCH 9

2. MATERIALS 10

2.1 FINE CHEMICALS AND REAGENTS 10
2.2 PLASMIDS 11
2.3 IMMUNOHISTOCHEMICAL STAINING 11
2.4 PRIMARY ANTIBODIES USED FOR WESTERN BLOT 11
2.5 SECONDARY ANTIBODIES USED FOR WESTERN BLOT 12
2.6 TAQMAN PROBES 12
2.7 TRANSCRIPTIONAL FACTORS FOR RT PCR 12
2.8 BUFFERS 12
2.9 READY FOR USE KITS AND SOLUTIONS 13
2.10 CELLS 16
2.11 ANIMALS 17
2.12 CONSUMABLES 17
2.13 INSTRUMENTS 18
2.14 SOFTWARE 19

3. METHODS 20

3.1 IN-VITRO WORK 20
3.1.1 HUMAN EMBRYONIC KIDNEY CELLS (HEK 293T) 20
3.1.2 ATRIAL MUSCLE CELL LINE (HL-1) 20
3.1.3 VENTRICULAR MUSCLE CELL LINE (H9C2 (2-1) (ATCC® CRL-1446™) 21
3.1.4 PLASMID CLONING 21
3.1.5 TRANSFECTION 22
3.1.6 EXTRACELLULAR FLUX ANALYZER 22
3.1.7 STAINING FOR MITOCHONDRIA AND REACTIVE OXYGEN SPECIES (ROS) 23
3.2 ANIMAL WORK 23
3.3 PROTEIN BIOCHEMISTRY 24
3.3.1 PROTEIN EXTRACTION AND ASSESSMENT OF PROTEIN CONCENTRATION 24
3.3.2 ELECTROPHORETIC PROTEIN SEPARATION (SDS-PAGE) 24
3.3.3 SAMPLE PREPARATION FOR GEL ELECTROPHORESIS 25
3.3.4 WESTERN BLOT AND PROTEIN DETECTION 25
3.4 AMINO ACID ANALYSIS 26
3.4.1 SAMPLE PREPARATION AND CALIBRATORS 26
3.4.2 HIGH PERFORMANCE LIQUID CHROMATOGRAPHY – MASS SPECTROMETRY (LC-MS/MS) 27
3.5 QUANTIFICATION AND STATISTICAL ANALYSIS 27

4. RESULTS 28

4.1 REGULATION OF UPSTREAM EFFECTORS OF PGC-1A 28
4.1.1 WESTERN BLOT FOR UPSTREAM EFFECTORS ON H9C2 CELL CULTURE 28
4.1.2 UPREGULATION OF AKT AND ERK IN UREA/OXALATE MODEL 31
4.2 OXIDATIVE STRESS BY UREA TREATMENT 33
4.2.1 DIFFERENCE IN REDUCED AMINO ACIDS IN THE MEDIA OF HL-1 CELLS 33
4.2.2 NO CHANGE OF THE NUMBER OF MITOCHONDRIA AND CONCENTRATION OF ROS 34
4.3 H9C2 CELLS SHOW SIGNIFICANT DIFFERENCE IN BASAL METABOLISM, UNCOUPLING AND RESERVE CAPACITY 38

5. DISCUSSION 44

5.1 UREMIA AND OXIDATIVE STRESS 44
5.2 UREA'S PATHWAY AFFECTING CELLULAR ENERGY RESILIENCE 46
5.3 UREMIA INCREASES OXYGEN CONSUMPTION 49
5.4 UREA-TREATED CELLS MAY HAVE AN INCREASED RESERVE CAPACITY 50
5.5 PGC-1A AND CARDIAC HYPERTROPHY 52

6. CONCLUSION AND LIMITATIONS 54

6.1 UREMIC CARDIOMYOPATHY – A PUZZLE WITH MANY PIECES 54
6.2 CLINICAL IMPLICATIONS: TARGET CARDIOPROTECTIVE PATHWAYS FOR ISCHEMIC RESILIENCE 56
6.3 CLINICAL IMPLICATIONS: CARBAMYLATED ALBUMIN - A POSSIBLE INDICATOR OF HEART FAILURE 56

7. SUMMARY 58

8. ZUSAMMENFASSUNG 60

9. LIST OF REFERENCES 62

10. APPENDIX 67

10.1 ABBREVIATIONS 67
10.2 ACKNOWLEDGEMENTS 70
10.3 CURRICULUM VITAE 71
10.4 PUBLICATIONS AND PRESENTATIONS 72
10.4.1 PUBLICATION 72
10.4.2 POSTER PRESENTATION 72
10.5 AFFIDAVIT/ EIDESSTATTLICHE ERKLÄRUNG 73

1. INTRODUCTION

For the last 20 years, Chronic Kidney Disease (CKD) has remained a major cause of death worldwide. Cardiovascular events even account for 40 to 50% of deaths in patients with CKD.(1, 2) Cardiac changes observed in CKD involve metabolic remodeling, compromised myocardial energetics, and loss of insulin-mediated cardioprotection. The entity of these symptoms describes Uremic cardiomyopathy (UCM).(3) This thesis focuses on the effect of urea on cardiomyocytes and on affected intracellular pathways that can be linked to the transcriptional coactivator peroxisome proliferator-activated receptor-γ (PPARγ) coactivator-1α (PGC-1α), an important orchestrator of intra-cellular energy metabolism.

1.1 Chronic Kidney Disease: Overview

The kidneys are important filtration devices of the human body. They are responsible for the body's volume control and for excretion of toxins and metabolic waste-products. Besides, the kidneys regulate electrolyte levels and have endocrine function (renin, erythropoietin, and calcitriol). The importance of these regulatory systems becomes apparent in the failing state – chronic kidney disease (CKD).

Damage to the kidney is mediated through two general processes: A trigger, such as a genetical alteration of kidney development or accumulation of immune complexes. And adaptational mechanisms like hypertrophy and hyperfiltration by the remaining functional nephrons. Long-term reduction of kidney mass causes these adaptions through hormones, cytokines, and growth factors. But these changes cannot compensate for the damaged nephrons for a longer period and therefore cannot equilibrate the elevated blood pressure and flow. This leads to a decreased glomerular filtration rate (GFR).(4)

CKD is defined by the International Society of Nephrology in the KDIGO (Kidney Disease: Improving Global Outcomes) Position Statement from 2012 as abnormalities of kidney structure or function, present for >3 months, with implications for health. These criteria can consist of either a decreased GFR <60 ml/min/1.73 m^2 or a different marker of kidney damage. This is illustrated in table 1.

Criteria for CKD (either of the following present for >3 months)	
Markers of kidney damage (one or more)	Albuminuria (AER ≥30 mg/24 hours; ACR ≥30 mg/g [≥3 mg/mmol]) Urine sediment abnormalities Electrolyte and other abnormalities due to tubular disorders Abnormalities detected by histology Structural abnormalities detected by imaging History of kidney transplantation
Decreased GFR	GFR <60 ml/min/1.73 m^2 (GFR categories G3a–G5)

Figure 1 | Criteria for chronic kidney disease; KDIGO 2012 clinical practice guideline for the evaluation and management of chronic kidney disease.(5)

In the latest clinical practice guideline, classification of CKD is based on cause, GFR, and albuminuria (CGA). Cause of CKD can be assigned based on presence or absence of systemic disease and pathologic changes located in the kidney. GFR category (G1 to G5) depends on the patient's GFR and CGA classification then sorts the patient into categories (A1 to A3), regarding their albumin excretion rate in 24 hours. This is shown in table 2.(5)

Prognosis of CKD by GFR and Albuminuria Categories: KDIGO 2012

GFR categories (ml/min/ 1.73 m²) Description and range				Persistent albuminuria categories Description and range		
				A1	A2	A3
				Normal to mildly increased	Moderately increased	Severely increased
				<30 mg/g <3 mg/mmol	30-300 mg/g 3-30 mg/mmol	>300 mg/g >30 mg/mmol
	G1	Normal or high	≥90			
	G2	Mildly decreased	60-89			
	G3a	Mildly to moderately decreased	45-59			
	G3b	Moderately to severely decreased	30-44			
	G4	Severely decreased	15-29			
	G5	Kidney failure	<15			

Figure 2 | Classification of Chronic Kidney Disease. The figure accounts for GFR category horizontally and albuminuria category vertically. Green: low risk for CKD(if no other markers of kidney disease, no CKD); Yellow: moderately increased risk for CKD; Orange: high risk for CKD; Red, very high risk for CKD.(6)

Symptoms of CKD vary in between patients from pruritus and sleep disorders to intestinal problems and pain. Lower stages of kidney disease are not associated with symptoms of decreased GFR but with the underlying kidney disease: Edema in patients with nephrotic syndrome, or secondary high blood pressure in polycystic kidney disease patients, for example. In higher stages nearly all organs are affected. Most evident complications include anemia and subsequently fatigue, loss of appetite and malnutrition, and damaged balance of electrolytes, acid-base state, and hormones (Calcitriol, Parathormone, Fibroblast-Growth-Factor 23). If a patient reaches kidney failure, toxins accumulate, and the patient is gravely limited in his every-day life. This condition is lethal if kidney replacement therapy is not initiated.(4, 7)

Chronic kidney disease is a highly prevalent condition. In 2017 global prevalence was estimated as 9.1% in the world's population. It varies between 3.31% in Norway and 17.3% in

northeastern Germany regarding all stages of CKD. Similar rates exist in China and the United States.(8, 9) Leading causes of chronic kidney disease show a global variance, too. In high-income and middle-income countries, diabetes (types 1 and 2) and hypertension are the main reasons. Diabetes accounts for 30 – 50% of all CKD and for 30.7% of CKD DALYs (DALY= disability-adjusted life-year, a measure of overall disease burden). In east Asia, eastern Europe, tropical Latin America, and western sub-Saharan Africa, high blood pressure accounts for the biggest number of cases of CKD. Also, in Asia, India, and sub-Saharan Africa, glomerulonephritis and unknown causes are more common. This can be explained by toxic effects of herbal medicines and environmental pollution of water, regarding heavy metals and organic compounds, such as pesticides.(9, 10)

In Germany, the leading causes for ESRD are diabetes, glomerulonephritis, and hypertensive nephropathy. In table 3, the different underlying diagnoses of patients undergoing dialysis treatment in the year 2006 are illustrated.(11)

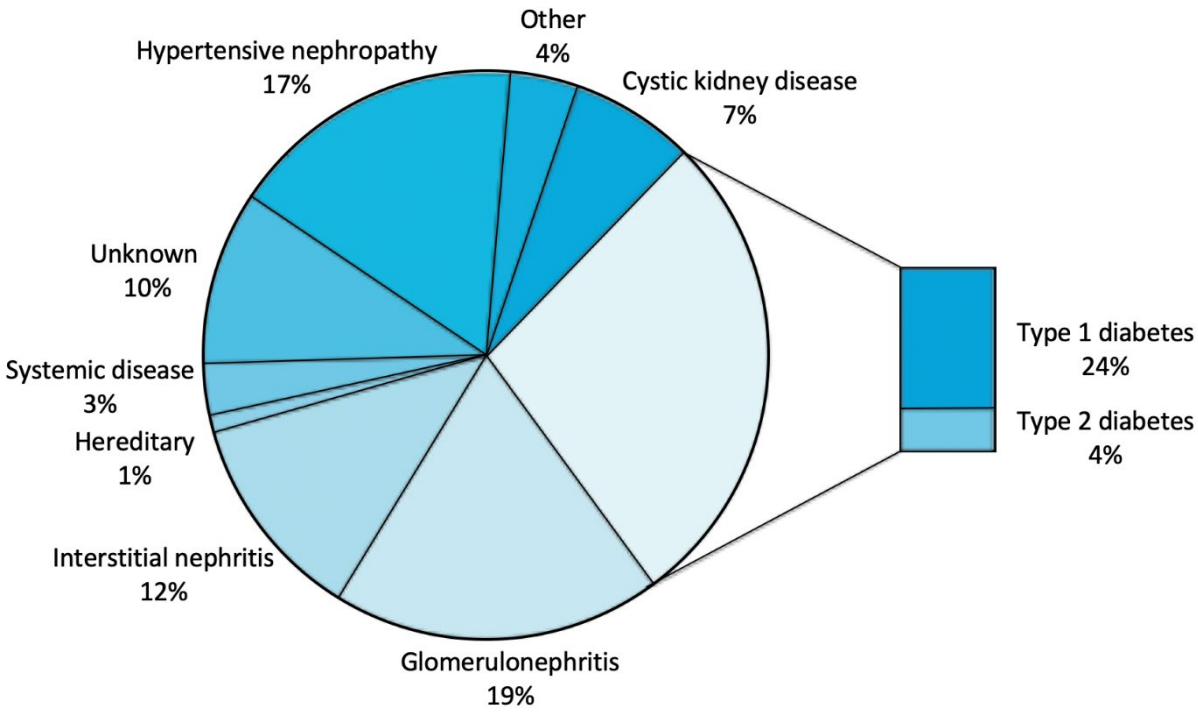

Figure 3 | Distribution of diagnoses of ESRD patients in Germany (2006, prevalence). Diabetes is the highest cause (28%), followed by glomerulonephritis (19%) and hypertensive nephropathy (17%). The Table has been translated from the original source; n = 48.535.(11)

The mortality of patients receiving dialysis can be divided into cardiovascular and non-cardiovascular causes, the latter including infections, malignancies, cachexia, withdrawal, suicide/refusal of treatment, and miscellaneous. For the first three years of dialysis treatment, these numbers have been compared by De Jager et al. in 2009. They found that "the increased risk of cardiovascular mortality in patients starting dialysis goes together with an equally increased risk of non-cardiovascular mortality" and underlined the importance of researching non-cardiovascular as well as cardiovascular causes. Their data is shown in table 4.(2)

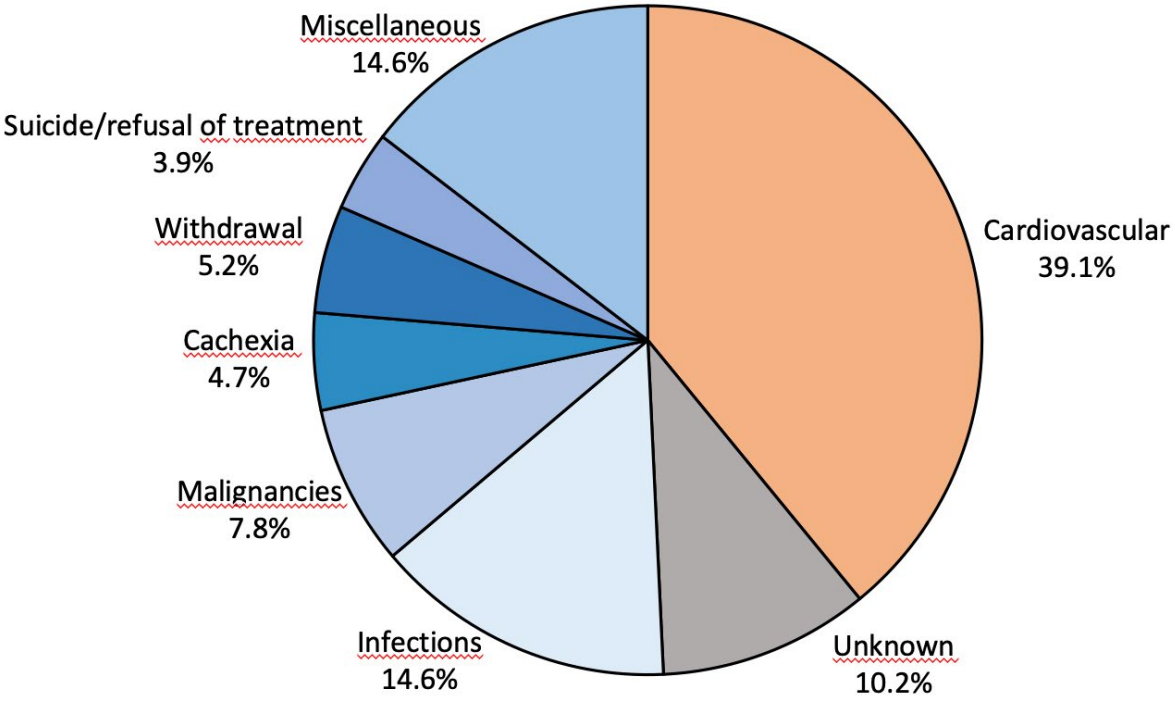

Figure 4 | Causes of death after first three years of dialysis. Data from the European Renal Association – European Dialysis and Transplant Association [ERA-EDTA] Registry (years 1994 to 2007); n = 123 407.

Cardiovascular events account for approximately 40 to 50% of deaths in patients with CKD and mortality due to cardiovascular disease (CVD) is 10 to 30 times higher in dialysis patients than in the general population.(2, 12, 13) In 2010, Matsushita et al. showed that the cardiovascular risk increases linearly with the decrease of the estimated GFR below the threshold of 75 ml/min/1.73m and especially in young patients, development of cardiac and vascular disease has shown to be rapid.(14, 15)

1.2 Pathophysiological changes in CKD: Uremic cardiomyopathy

When kidney function declines, the kidneys are incapable of excreting enough water and waste products (uremic toxins). Both these toxins and endocrine failure (e.g., deficiency of erythropoietin and vitamin D, or excess of parathyroid hormone) cause major structural and functional changes to the heart and the vascular system, resembling all aspects of an accelerated ageing process and latent cardiac failure. The vascular tree can be affected by both atherosclerosis and arteriosclerosis with lipid rich plaques and abundant media calcification. It has been shown that patients undergoing dialysis have pronounced atherosclerosis with specific calcification and lipid patterns. Furthermore, marked fibrous or fibro-elastic thickening of elastic and muscular arteries with a loss of elastic fiber content are linked to CKD. This causes increased vascular stiffness and pronounced peripheral artery disease.(14)

In the heart, the changes include impaired angio-adaption, myocardial micro-arteriopathy, myocardial fibrosis and left ventricular hypertrophy (LVH). The entity of these symptoms has been termed uremic cardiomyopathy (UCM), with LVH being the primary manifestation.(14, 16) Apart from increased pre- and afterload, the parathyroid hormone (PTH) seems to play a role on LVH, interstitial fibrosis and cardiac arterioles, as its concentration correlates with cardiac morbidity and cardiac death in dialysis patients. Other authors suggest an intensification of cardiac changes by the renin-angiotensin-aldosterone system (RAAS) and the endothelin (ET) system. Especially ET-1 correlates closely with the development of LVH.

Another factor that interferes with oxygen supply of the heart muscle is the reduction of capillary density. This lack of oxygen makes the heart more susceptible to ischemic damage and may increase the cardiac risk in uremic patients. This rarefaction also occurs in different types of hypertrophy, but is significantly more pronounced in uremia.(17)

1.3 Urea – just metabolic waste?

Urea is produced in a set of biochemical reactions, mainly in the liver and the kidney, to prevent toxic levels of ammonium, which develop from the breakdown of amino acids. Then, urea is eliminated through the kidneys. The physiologic plasma concentration averages no higher than 416 µM for male, and 339 µM for female individuals.(4, 18)

Physiologically, a cell needs to get rid of certain toxins that originate from its metabolism. If this buffering capacity is exceeded by abnormal cell metabolism, aggressive peroxides and free radicals can no longer be eliminated. The term “oxidative stress” reflects this imbalance in the redox state of the cells that can cause damage to all cellular components. It mainly consists of reactive oxygen species (ROS) such as peroxides, superoxides and hydroxyl radicals. The induction of oxidative stress has impaired cardiomyocyte viability in previous studies and reduction of oxidative stress has led to augmented survival of various cell types.(19, 20)

In the past, the effect of elevated urea in CKD was neglected. Blood urea concentrations of less than 50 mM were well tolerated in dialysis and the HEMO study demonstrated in 2002 that increasing urea reduction rate from 66% to 75% did not alter survival in patients with an increased dialysis dose.(21, 22) However, patients with ESRD displayed elevated levels of oxidative stress, which reflects an imbalance between the generation of reactive oxygen species (ROS) and the cellular ability to detoxify reactive intermediates or to repair resulting damage. Recent data showed that non-physiologic levels of urea lead to increased ROS production and an elevated level of 8-oxoguanine, a marker of oxidative stress.(23-25) Mitochondrial ROS production was triggered by exposing human aortic endothelial cells to 20 mM urea, a concentration found in chronic renal failure.(26) These results suggest an important effect of urea on the mitochondria of endothelial cells.

1.4 PGC-1α – orchestrator of mitochondrial metabolism

The question arises what connects urea to an impaired mitochondrial metabolism. The transcriptional coactivator peroxisome proliferator-activated receptor-γ (PPARγ) coactivator-1α (PGC-1α) is considered an important regulator of mitochondrial content and orchestrator of intra-cellular energy metabolism.(27, 28)

PGC-1α was first discovered due to its importance in thermogenesis. Its mRNA expression was highly elevated upon cold exposure in both brown fat and skeletal muscle, key thermogenic tissues, and connected to upregulation of PPARγ and uncoupling protein-1 (UCP-1, also called thermogenin).(29) Aside from cold temperature, it is induced by physical exercise and mediates muscle adaption.(30, 31) Soon, PGC-1α was linked to mechanisms controlling mitochon-

drial biogenesis and respiration. The nuclear genome encodes most proteins found in the mitochondria. PGC-1α and PGC-1β, a related coactivator, induce the transcription of most of these genes. This includes the proteins necessary for the electron transport chain, the Krebs (TCA) cycle, and those involved in the β-oxidation of fatty acids.(28, 32, 33)

In the cardiomyocyte, PGC-1α and β are highly expressed. This is in line with the high metabolic activity of this cell type.(28) PGC-1α levels correlated with cardiac oxidative capacity (34) and hearts from PGC-1α KO mice had reduced mitochondrial enzymatic activities, decreased levels of ATP and their hearts had a diminished ability to increase work output.(35) Constitutive cardiac PGC-1α overexpression in mice resulted in uncontrolled mitochondrial proliferation, leading to dilated cardiomyopathy.(36) In culture, PGC-1α increased mitochondrial number, upregulated expression of mitochondrial enzymes, and increased rates of fatty acid oxidation and coupled respiration.(37, 38)

1.5 Objective of research

Cardiac events account for a major part of deaths in CKD patients. These patients show metabolic changes, which could be caused by altered regulation of PGC-1α. Our objective was to investigate the signaling pathways connecting uremia, PGC-1α, and myocardial dysfunction. We also investigated the effects of urea on cardiomyocyte metabolism, as we suspect urea to cause an alteration on mitochondrial viability.

Hypothesis:

PGC-1α plays a role in the cardiac changes seen in uremic cardiomyopathy.

To test our hypothesis, we designed the following experiments:

A) Treatment of endothelial cells and cardiomyocytes with high-physiological concentration of urea in a time course from 30 minutes to 48 hours, to distinguish short-term activation (e.g. phosphorylation) from long-term alterations (e.g. transcription). To consider osmotic effects, we included a glucose-treated control group (25 mM).(39) As urea can spontaneously transform into cyanate, we included a cyanate-treated group to eliminate the chance, that we solely investigate the effect of cyanate.

B) Analyzing heart tissue of mice which were fed a high-urea/oxalate diet to simulate kidney failure. This diet is used to induce stable stages of CKD in mice.(40)

2. MATERIALS

2.1 Fine chemicals and reagents

Acetic acid	Fluka
Acetonitrile	Laboratory stock
BioAcryl-P (30%)	Boston BioProducts
Agarose	Sigma
Ammonium Persulfate (APS)	Sigma
Amidoblack 10B	Bio-Rad
Chloroform	Sigma-Aldrich
D-Glucose	Sigma-Aldrich
D-Mannitol	Fischer Scientific
Dimethyl Sulfoxide (DMSO)	Fischer BioReagents
Ethanol	Sigma-Aldrich
Fetal Bovine Serum (HL-1 screened)	Sigma-Aldrich
Formaldehyde	Fischer Chemical
Isopropanol	Sigma-Aldrich
L-Ascorbic Acid	Sigma-Aldrich
L-Glutamine	Cellgro
Methanol	Sigma-Aldrich
Norepinephrine	Sigma-Aldrich
Potassium cyanate	Sigma-Aldrich
Sodium pyruvate	Laboratory stock
Standard Fetal Bovine Serum	HyClone
Tetramethylethylenediamine (TEMED)	Sigma
TRIzol® Reagent	Ambion
Urea	Fischer Scientific

2.2 Plasmids

PGC-1α promoter 2kb luciferase #8887	addgene
pcDNA-f:PGC1 #1026	addgene
FLAG-FOXO3a WT #8360	addgene
pSG5 PPARα #22751	addgene

2.3 Immunohistochemical staining

MitoSOX™ Red mitochondrial superoxide indicator	Invitrogen
MitoTracker™ Red CM-H2XRos	Invitrogen
MitoTracker™ Green FM	Invitrogen
DAPI (4,6-diamino-2-phenylindole, dihydro-chloride)	Invitrogen

2.4 Primary antibodies used for western blot

PGC-1α	Laboratory stock
PPARγ	Laboratory stock
pFOXO3α (p-FOXO01 (T24)/FOXO03a)	Cell Signaling Technologies
Akt (Akt (pan)(C67E7))	Cell Signaling Technologies
pAkt (P-Akt (S473) (193H12))	Cell Signaling Technologies
Erk (p44/42 MAPK (Erk1/2))	Cell Signaling Technologies
pErk (P- p44/42 MAPK (Erk1/2))	Cell Signaling Technologies
pp38 (p38 MAPK (D13E1)XP®)	Cell Signaling Technologies
JNK (SAPK/JNK)	Cell Signaling Technologies
β-Actin	Laboratory stock

2.5 Secondary antibodies used for western blot

Peroxidase conjugated AffinPure F(ab')2 rabbit	Jackson ImmunoResearch
Anti-mouse antibodies	Laboratory stock

2.6 TaqMan probes

TaqMan® Gene Expression Assays	Applied Biosystems
TaqMan® Fast Advanced Master Mix	Applied Biosystems
TaqMan® Assay probes (Mm01208835_m1 Ppargc1; Mm00725448_s1 Rplp0)	Applied Biosystems

2.7 Transcriptional factors for RT PCR

PPARG coactivator 1 alpha (#4331182)	Thermo Fischer Scientific

2.8 Buffers

TBS-Tween-20 Washing Buffer(10X)	Tris 500 mM NaCl 1.5 M Tween-20 1%	Boston BioProducts
Tris-Glycine-SDS Running Buffer (10X)	Tris base 250 mM Glycine 1.92 M SDS 1%	Boston BioProducts
Transfer Buffer (10X)	Tris base 0.25 M Glycine 1.92 M	Boston BioProducts
Destaining Buffer	Methanol 45% Acetic acid 10%	Boston BioProducts

SDS Sample Buffer (4X)	Tris-HCL 250 mM SDS 8% Glycerol 40% bME 8% Bromophenol 0.02%	Boston BioProducts
Stacking Buffer	Tris-Base 0.5 M SDS 0.4%	Boston BioProducts
RIPA Buffer (5X)	Tris-HCl 250 mM NaCl 750 mM NP-40 5% Sodium deoxycholate 2.5% SDS 0.5%	Boston BioProducts

2.9 Ready for use kits and solutions

Amidoblack solution	Methanol 40ml Acetic Acid 10ml Amidoblack 0.1g H_2O 50ml	Laboratory stock
Amino acid solution		Sigma-Aldrich
Ampicillin 50 mg/ml		Laboratory stock
Claycomb Medium	Total protein 261 mg/l Bovine albumin 48.85 mg/l Nones- sential amino acids 0.1 mM Fetuin 165 mg/l Transferrin 31.8 mg/l Retinoic acid 300 µg/l Human insulin (recombinant) 0.1 µg/l Long R^3IGF-1 (recombinant) 0.1 µg/l Long EGF (recombinant) 0.1 µg/l	Sigma-Aldrich

	Cholesterol 1.96 mg/l Linolic acid 0.78 mg/l γ-Oleyl-β-pal-α-phosphatidylcholine 1.96 mg/l Ascorbic acid 0.3 mM	
DEPC-Treated Water		Ambion
Dulbecco's Modified Eagle's Medium (DMEM)	Glucose 4500 mg/l L-glutamine 4500 mg/l Sodium bicarbonate 4500 mg/l	Sigma
Endothelium Cell Basal Medium-2 Bulletkit	EBM-2 Basal Medium 500 ml FBS 10 ml Hydrocortisone 0.2 ml hFGF 0.2 ml VEGF 0.5 ml R3-IGF-1 0.5 ml Ascorbic Acid 0.5 ml hEGF 0.5 ml GA-1000 0.5 ml Heparin 0.5 ml	Lonza
Ethidium Bromide Solution		Bio-Rad
Fibronectin (1 mg/ml)		Sigma-Aldrich
Formaldehyde load dye		Ambion
Gelatin solution 2%		Sigma
Hanks' Balanced Salt Solution (HBSS)		Gibco
Isotopic Standards		Cambridge Isotopics
LB-Medium Miller	Trypton 1% Yeast extract 0,5% NaCl 1%	Boston BioProducts

L-Glutamine 200 mM Solution		Cellgro
L-Glutamine-Penicillin-Streptomycin solution	L-glutamine 200 mM	Penicillin 10000 units
Streptomycin 10 mg/ml		Sigma
Lipofectamine® 2000		Invitrogen
Lipofectamine® 3000		Invitrogen
MOPS Electrophoresis Buffer		Fischer BioReagents
NorthernMax® MOPS Gel Running Buffer		Ambion
Nuclease-Free Water		Ambion
Opti-MEM® I Reduced Serum Medium		Thermofisher
Penicillin-Streptomycin Solution	Penicillin 5000 I.U./ml Streptomycin 5000 µg/ml	Cellgro
Phosphate Buffered Saline	Na_2HPO_4 (10 mM) KH_2PO_4 (2 mM) KCL (2.7 mM) NaCl (137 mM)	Boston BioProducts and Gibco
Phosphatase Inhibitor Cocktail 2		Sigma
Ponceau S solution	PonceauS 0.1% Acetic acid 5%	Sigma-Aldrich
Protease Inhibitor		Laboratory stock
PMSF		Laboratory stock
DTX		Laboratory stock
Pierce® BCA Protein Assay	BCA Reagent A (sodium carbonate, sodium bicarbonate, bicinchoninic acid and sodium tartrate in 0.1 M sodium hydroxide)	Thermo Scientific

	BCA Reagent B (4% cupric sulfate) Albumin Standard Ampules 2mg/mL (bovine serum albumin (BSA) at 2 mg/mL in 0.9% saline and 0.05% sodium azide)	
Precision plus protein ladder		Bio-Rad
RNaseZap™		Invitrogen
RNeasy® Mini Kit (250)		Qiagen
SuperSignal® West Pico Chemiluminescent Substrate		Thermo Scientific
SuperSignal® West Femto Trial Kit		Thermo Scientific
Trypsin-EDTA Solution	Trypsin 2.5 g EDTA 0.2 g 4 Na per liter of HBSS with phenol red	Sigma
Western Blocker Solution™ Solution		Sigma
XF Base Medium		Agilent Technologies
XF cell mito stress test kit		Agilent Technologies

2.10 Cells

HL-1 Cardiac Muscle Cell Line	Sigma-Aldrich
H9c2(2-1) (ATCC® CRL-1446™)	ATCC
HEK 293T	Laboratory stock
DH5α™ Competent E. coli	Invitrogen

2.11 Animals

8-week-old male FVB mice were obtained from Charles River Laboratories. IACUC-approved protocol no. 059–2015 / 101118 (Animal Welfare Assurance #A3153-01).

2.12 Consumables

1.5 ml Microcentrifuge Tube	SealRite
1.5 ml sterile Microcentrifuge Tube	Fischerbrand
2.0 ml Microcentrifuge Tube	USA Scientific
Disposable Cell Scraper	Fischerbrand
Filter paper	Bio-Rad Laboratories
Filter sterile pipets	USA scientific
Tube Top Filter 50 ml	Corning
0.2 µm PES for filtration 500 ml	Autofil
Mini-PROTEAN® Precast Gels	Bio-Rad Laboratories
Immobilon®-FL Transfer Membranes	Merck Millipore
Insulin Syringes 0.37x12.7 mm	Exel
Luna HPLC column (100x3.0 mm, 2.6 µm)	Phenomenex Inc.
MicroAmp® Fast optical 96-Well 0.1 ml plate	Applied Biosystems
Mini-Protean® Glass plates 1.0 mm	Bio-Rad
Mini-Protean® Glass plates 1.5 mm	Bio-Rad
Corning 3506 6 well	Corning
Corning 3527 24 well	Corning
Corning 3548 48 well	Corning
Corning Flask 75 cm^2	Corning
Corning 43029 100mm Dish	Corning
XF24 V7 cell culture microplate	Seahorse Bioscience
XF96 V3 cell culture microplate	Seahorse Bioscience

PCR Plate 96 well, PP, 0.3 ml non-skirted	Fischerbrand
Pipettes and Tips	Laboratory stock
RNase-Free 0.2 ml PCR Tubes w/caps	Ambion
50 ml Conical Centrifuge Tubes	Thermo Scientific
15 ml Conical Centrifuge Tubes	Thermo Scientific

2.13 Instruments

7500 Fast Real-Time PCR System	Applied Biosystems
API 5000™ System	AB Science
Bel-Art™ SP Scienceware™ Liquid Nitrogen-Cooled Mini Mortar	FischerScientific
Blotting chamber: Mini PROTEAN® Tetra Cell	Bio-Rad Laboratories
Dry Bath Incubator MK-20	TSZ Scientific
Easycast B1A-BP gel electrophoresis chamber	Thermo Scientific
Electrophoresis Power Supply Gibco BRL	Life Technologies
GeneAmp® PCR System 2700	Applied Biosystems
IncuBlock™	Denville Scientific inc.
Invitrogen™ EVOS™ FL Cell Imaging System	Thermo Scientific
Freezing container	Nalgene
Isotemp Heat Block	Fischer Scientific
MicroMax® Centrifuge	IEC
Microwave theGenius inverter	Panasonic
MilliQ	Millipore
Mini Centrifuge	Fischer Scientific
NanoDrop 2000c Spectrophotometer	Thermo Scientific
ORBI Shaker MP	Benchmark
PowerPac® Basic	BioRad

SpectraMax 190	Molecular Devices
SpectraMax M5	Molecular Devices
Thermomixer	Eppendorf
The Belly Dancer	Stovall Life Science
ThermoScientific myECL Imager	Thermo Scientific
Vortex Genie 2	Scientific Industries
XF 24 Extracellular Flux Analyzer	Seahorse Bioscience
XFe 96 Extracellular Flux Analyzer	Seahorse Bioscience
XF Prep Station	Seahorse Bioscience

2.14 Software

Adobe Photoshop

Analyst 1.6

ImageJ

Microsoft Office 365

NanoDrop2000

Thomson EndNote

Wave Seahorse XF

3. METHODS

3.1 In-vitro work

3.1.1 Human Embryonic Kidney Cells (HEK 293T)

The 293T cell line is a highly transfectable derivate of Human Embryonic Kidney 293 cells. The 293T cells express the Large T antigen, important for replicating plasmids containing a SV40 origin of replication.

We grew the cells on 100 mm dishes in an incubator containing 5% CO_2 at 37^{o}C and used DMEM growth medium, which we filtered to avoid contamination.

DMEM medium:	DMEM	89%
	FBS	10%
	Penicillin/Streptomycin	1%

When the cells reached full confluence, they were detached by incubating them at 37^{o}C with 1.3 ml Trypsin/EDTA solution. The detached cells were repeatedly pipetted to avoid clumping and incubated on new dishes overnight.

3.1.2 Atrial Muscle Cell Line (HL-1)

HL-1 cells (Sigma-Aldrich) are immortalized atrial mouse cardiomyocytes able to continuously divide and spontaneously contract while maintaining a differentiated cardiac phenotype. For proliferation, we grew the cells on dishes that were coated with gelatin/fibronectin solution containing 0.04% gelatin and 20 µg/ml fibronectin. The solution was filter-sterilized using a 0.22 µm filter and left on the cell culture dish for at least one hour at 37^{o}C before using the dishes for cell culture. Media was prepared as recommended by the manufacturer using the following ingredients:

Norepinephrine 10 mM:	Distilled Water	100 ml
	Ascorbic acid	0.59 g
	Norepinephrine	320 mg
Supplemented Claycomb Medium:	Claycomb Medium	87 ml
	FBS	10 ml
	Penicillin/Streptomycin	1 ml
	Norepinephrine 10 mM	1 ml
	L-Glutamine 200 mM	1 ml

Supplemented Claycomb Medium was filter-sterilized and wrapped in aluminum foil, since the medium is extremely light sensitive. Therefore, cell work was done leaving the hood lighting off. Cells were fed daily and passaged at high confluence following the protocol provided by SAFC®.

3.1.3 Ventricular Muscle Cell Line (H9c2 (2-1) (ATCC® CRL-1446™)

H9c2(2-1) cells are a subclone of the original clonal cell line derived from embryonic BD1X rat heart tissue. The myoblast cells were cultured in DMEM medium containing 10% FBS. For passage, we followed the protocol provided by ATCC® and kept the cells beneath 70% confluence for expansion.

3.1.4 Plasmid cloning

We used DH5α competent E. coli cells to clone plasmid vectors following the protocol provided by Invitrogen. The successful transfection was controlled by antibiotic selection on ampicillin containing LB plates. A single colony was transferred into 100 ml of LB-Medium Miller containing ampicillin at 50 µg/ml and incubated at 120 rpm at 37^{o}C overnight. The next day, the plasmids were extracted using EndoFree® Plasmid Maxi Kit (Qiagen) and subsequently stored at -20^{o}C.

3.1.5 Transfection

Transfection was performed on HEK 293T cells in 6well plates growing in DMEM medium without antibiotics. We followed Lipofectamine® 2000 DNA Transfection Reagent Protocol. The successful transfection was confirmed by western blot.

3.1.6 Extracellular Flux Analyzer

We measured the oxygen consumption rate (OCR) and extracellular acidification rate (ECAR) in live cells using Seahorse Bioscience XF24 Extracellular Flux Analyzer (Seahorse Bioscience). Cells were seeded into quadruplicate wells of XF24 V7 cell culture plates (Seahorse Bioscience). The next day, the medium was changed to XF assay medium (Seahorse Bioscience), supplied with 10 mM glucose, 1 mM pyruvate and 2 mM glutamine. After a one-hour incubation in a non-CO2 incubator, OCR and ACAR were measured three times. Then, measurements were taken as the cells were treated in four conditions: (1) no additives to measure basal levels; (2) 1 µM oligomycin to reversely inhibit ATP synthase (complex V) and reveal glycolysis alone; (3) 0.3 µM Carbonyl cyanide-4-(trifluoromethoxy)phenylhydrazone (FCCP), an uncoupling agent, induces maximal respiration; (4) 0.5 µM rotenone/antimycin A, a mitochondrial poison and Complex I inhibitor, to show non-mitochondrial respiration.

We used Pierce® BCA Protein Assay to adjust the results to the number of cells existing in each well. Cells were lysed in 10 µl RIPA buffer for 10 minutes on a shaker and we then added 200 µl of BCA solution and incubated the reaction at 37^{o}C for 30 min. Diluted albumin in the concentrations 0.125 mg/ml, 0.5 mg/ml, 1 mg/ml, 2 mg/ml and 4 mg/ml was used for calibration. SpectraMax 190 was utilized to measure absorbance. We made use of the Seahorse software “Wave” to normalize for protein quantity and plot the results.

3.1.7 Staining for mitochondria and Reactive oxygen species (ROS)

MitoTracker Green FM (ThermoFisher) is a reduced dye, that fluoresces upon oxidation and stains mitochondria in live cells. It was used at a concentration of 500 nM. MitoSOX™ Red reagent (ThermoFisher) that specifically targets mitochondria and produces fluorescence only upon oxidation by superoxides. We used it in a concentration of 5 µM. To show the integrity of the nucleus, we used Hoechst® nucleid acid stain.

Staining dyes were diluted to the above-mentioned concentration in HBSS. Cells were treated with MitoTracker for 45 min and with MitoSox for 10 min. The staining solution was then replaced with warm HBSS. Cells were examined using EVOS™ FL Cell Imaging System (Invitrogen).

3.2 Animal work

All procedures were performed according to the IACUC-approved protocol no. 059–2015 / 101118 (Animal Welfare Assurance #A3153-01). 8-week-old male FVB mice were obtained from Charles River Laboratories and housed in groups of 3-5 mice in standard housing conditions with unlimited access to food and water. One group (n=6) of mice was given a standard diet as control group and a larger group (n=21) was given an oxalate diet for 3 weeks. The oxalate diet (catalog no. TD.110105, Envigo Teklad Diets, NJ, USA) was prepared by adding 0.67% (6.7 g/kg) sodium oxalate to a calcium deficient standard diet (catalog no. TD.95027) as reported elsewhere.(41) Mice with baseline mild/moderate crystal-induced nephropathy were maintained with western-type diet (catalog no. D12492, Research Diets, Inc. NJ, USA) and 50 g/L urea with or without taurine 10 g/L (as carbamylation scavenger) in their drinking water for 8 weeks. Control animals were similarly treated with oxalate but only fed western-type diet. Animals to be studied were randomly chosen.

3.3 Protein Biochemistry

3.3.1 Protein extraction and assessment of protein concentration

Heart tissue was homogenized using a Liquid Nitrogen-Cooled Mini Mortar (Fisher Scientific) and resolved in RIPA buffer. After an incubation on ice for 1 hour, we homogenized the samples by passing them 7 times through Insulin Syringes (Exel). Insoluble material was pelleted by centrifugation at 10000 X G for 10 minutes. Samples from cell culture were first washed with ice-cold PBS and harvested in 1 ml RIPA buffer. Protein was quantified using SpectraMax M5 Flurometer (Molecular Devices). Samples were stored at -20^{o}C.

3.3.2 Electrophoretic protein separation (SDS-PAGE)

Proteins were separated in a polyacrylamide gel electrophoresis (PAGE) based on their molecular weight. We used Mini-PROTEAN® Precast Gels (Bio-Rad) and self-made gels. For the self-made gels we used following formulae:

Resolving gel:	ddH_2O	15,8 ml
	Acrylamide (30%)	13,3 ml
	Running Buffer	10,4 ml
	APS	400 µl
	TEMED	40 µl
Stacking gel:	ddH_2O	13,2 ml
	Acrylamide (30%)	5 ml
	Running Buffer	6,5 ml
	APS	250 µl
	TEMED	25 µl

Gels were manufactured in a Mini-gel chamber (Bio-Rad). The resolving gel was polymerized between two glass plates (Bio-Rad) and covered with isopropanol to lower surface tension and straighten the gel. The stacking gel was loaded onto the resolving gel and inserted with a comb to spare the sample wells. The chamber was filled with running buffer and the samples were loaded into the wells. To determine the protein size, we filled the first well with Precision

plus protein ladder (Bio-Rad). Remaining wells were filled with SDS sample buffer to avoid diffusing the bands from neighboring wells to the empty wells. With four gels in the chamber, 60 mA constant electric current was set for 15 min and then increased to 100 mA for an hour.

3.3.3 Sample preparation for gel electrophoresis

Proteins in the RIPA-lysate were heat-denatured in SDS Sample buffer (2X) containing β-mercapthoethanol (β-ME). The high temperature, β-ME and SDS assured protein denaturation and breakdown of the disulfide bridges. The anionic SDS molecules bind to the polypeptides and outweigh their intrinsic charge. The gel acts as a micro-sieve, thus small proteins wander along the electric field at higher velocity, compared to higher molecular proteins. This method secures protein separation due to molecular mass and not due to interfering effects of protein-intrinsic charge.

3.3.4 Western blot and protein detection

PVDF membranes were activated in methanol on a shaker for 1 min. SDS-PAGE-separated proteins were transferred from the gel onto the membrane by wet blotting. Filter papers, membrane and gel were soaked in transfer buffer and stacked vertically in a transfer chamber. The chamber was filled with transfer buffer and a cool pack was added to reduce heat. The chamber was set to constant 110 Volt for 90 min and transfer efficiency was evaluated by unspecific protein staining using Amidoblack solution or Ponceau S. The color was removed with destaining buffer and wash buffer afterwards.

The membrane was blocked for 1 hour using blocking buffer to prevent unspecific antibody binding. For detection of the target proteins, we incubated the membrane overnight at 4^0C in blocking buffer containing the primary antibody in a dilution recommended by the manufacturer. After removing the primary antibody and three 10 minutes washing steps in washing buffer, the secondary antibody directed against the primary antibody was added in a 1:3000-dilution in blocking buffer. After five additional washing steps, the membrane was incubated in an enhanced chemiluminescent (ECL) HRP substrate for 5 minutes which was mixed directly

before usage according to manufacturer's recommendation. Chemiluminescence was detected using Thermo Scientific myECL Imager and band density was evaluated using ImageJ® (NIH).

3.4 Amino acid analysis

3.4.1 Sample preparation and calibrators

Cell culture media was collected, and cells were lysed with methanol. 20 µl of isotopic standards (Cambridge isotopes) and 160 µl of acetonitrile (ACN) were added to 20 µl of media or cell lysate. Isotopic standards did not include glutathione, but we expected the sensitivity to be sufficient. We also included iodoacedamide to prevent oxidation. The liquid was vortexed and subsequently centrifuged at 10000 rpm for 5 minutes. 100 µl of the supernatant was collected for LC-MS/MS.

Standard amino acid solution (100 µMol of each standard amino acid dissolved in HCl, SigmaAldrich) was diluted in milliQ water and used for calibration. The solution included 100 µMol homocysteine, cysteine, cysteinylglycine, and glutathione.

3.4.2 High performance liquid chromatography – mass spectrometry (LC-MS/MS)

Liquid chromatography was performed using Luna HPLC column (100x3.0 mm, 2.6 µm) (Phenomenex Inc.) with a flow rate of 0.5 ml/min at 50^0C. Mobile phase consisted of 90% ACN, 10 mM ammonium formate and 10% formatic acid. Concentration of ACN was subsequently decreased to 50%.

Samples were monitored using API 5000™ System (AB Science) triple quadrupole equipped with an electrospray ionization source. For system control and data analysis, we used Analyst 1.6 software. The API 5000™ System was operated in ESI-positive mode and capillary voltage was set to 2.5 kV. The nebulizer used nitrogen at a desolvation temperature of 450^0C and desolvation gas flow of 15 l/h. Ion source gas 1 and 2 (GS1 and GS2) were set to 40 l/h. The collision chamber contained nitrogen, collision energy was set to 25 and entrance potential and declustering potential to 15 and 100, respectively. Dwell time was fixed at 50 ms. The mass spectrometer was operated in multi reaction monitoring mode and validated for linearity and precision.

3.5 Quantification and statistical analysis

Data is presented as mean ± SD. For comparison of two groups, the two-tailed Student's t-test was used in Microsoft Excel® (2007). Comparison of more than two groups was done by one-way ANOVA followed by the Tukey's Multiple Comparison test using VassarStats website (Ref: Lowry, Richard. VassarStats: Website for Statistical Computation. http://vassarstats.net/ (last accessed 27 October 2020)). P values < 0.05 were considered statistically significant.

4. RESULTS

4.1 Regulation of upstream effectors of PGC-1α

4.1.1 Western blot for upstream effectors on h9c2 cell culture

Figures 5 to 8 present quantitative western blot results for upstream effectors of PGC-1α: The protein kinases Akt and Erk. Our results showed an increased expression of Erk by urea-treatment, although the total amount of pErk remained unchanged. Akt on the other hand showed a significant increase of its phosphorylated form in the urea-treated group.

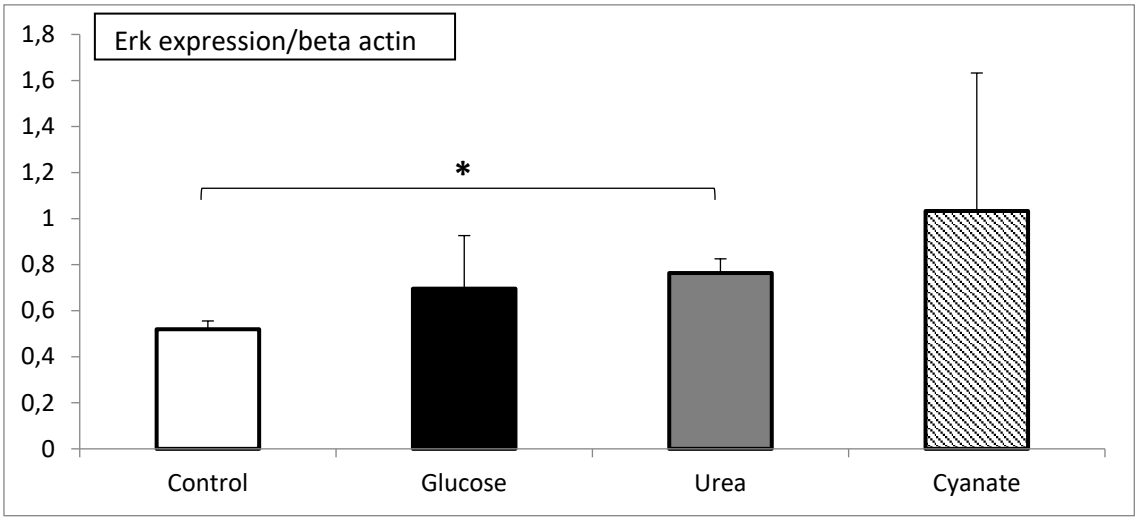

*Figure 5 | Increased Erk expression in urea-treated h9c2 cells. Western blot analysis of h9c2 cells that were treated with glucose, urea, or cyanate for 30 minutes. Erk expression was measured and compared to beta actin as a loading control. Erk expression was significantly elevated in the urea-treated group. (Mean ± SD; n = 3 – 4 per group; * = p < 0.05 vs the control group; one-way ANOVA followed by Tukey's post-hoc test.)*

Figure 5 shows a significant increase ($p < 0.05$) of Erk protein expression (0.76, 95%-CI[0.69, 0.83]) in comparison to the control group (0.52, 95%-CI[0.48, 0.56]), although the trend towards increased expression of Erk can be seen in the glucose group as well as in the cyanate group. Furthermore, figure 6 shows that there is no clear change of Erk phosphorylation.

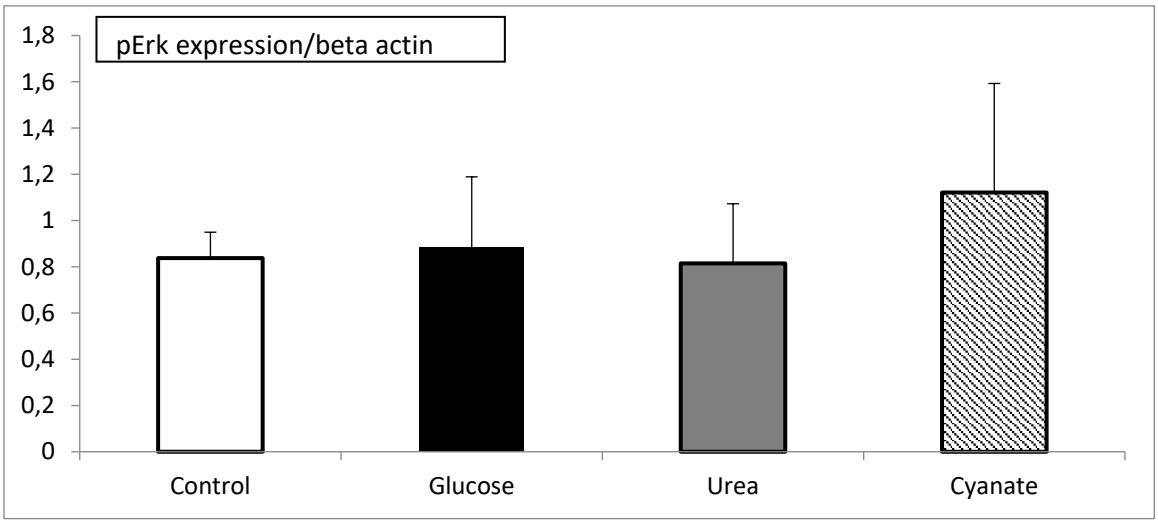

Figure 6 | No significant trend of phosphorylated Erk in urea-treated h9c2 cells. Western blot analysis of h9c2 cells that were treated with glucose, urea, or cyanate for 30 minutes. pErk expression was measured and compared to beta actin as a loading control. There was no apparent trend regarding the concentration of pErk in between the four groups. (Mean ± SD; n = 3 – 4 per group; one-way ANOVA followed by Tukey's post-hoc test.)

To investigate the rate of phosphorylation of Erk, we measured the phosphorylated Erk (pErk) and compared it to the total amount of Erk. We found that this ratio has significantly decreased ($p < 0.05$) in the urea group (0.98, 95%-CI[0.72, 1.24]) compared to the control group (1.63, 95%-CI[1.26, 1.99]). The results can be seen in figure 7.

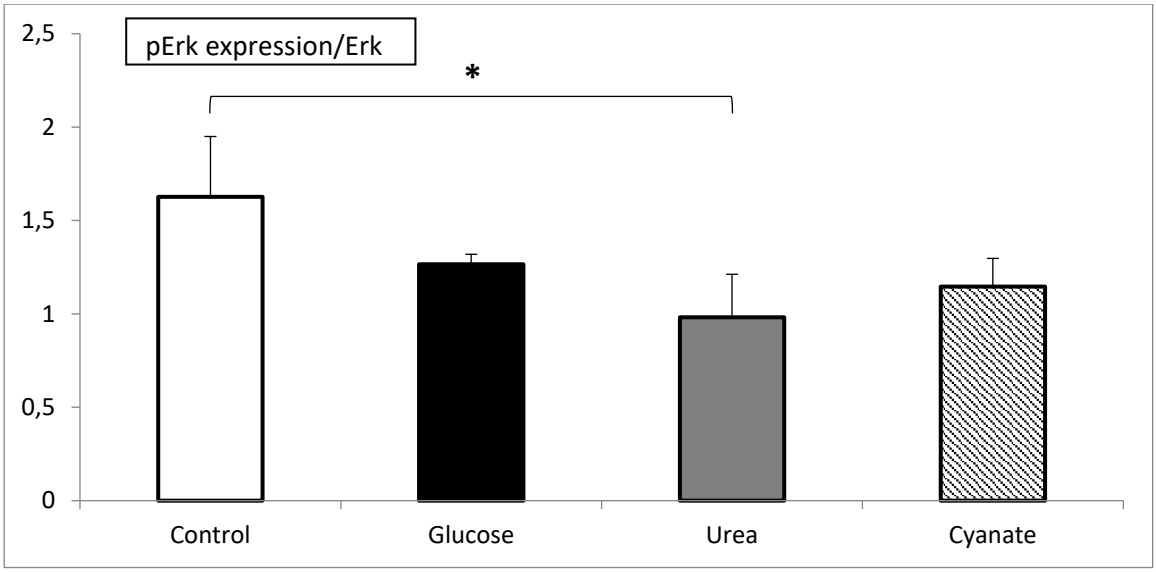

*Figure 7 | Downregulation of pErk compared to total Erk in the urea-treated group. Western blot analysis of h9c2 cells that were treated with glucose, urea, or cyanate for 30 minutes. Erk expression was measured and compared to total Erk. pErk expression was significantly downregulated in the urea-treated group. (Mean ± SD; n = 3 – 4 per group; * = p < 0.05 vs the control group; one-way ANOVA followed by Tukey's post-hoc test.)*

Phosphorylation of Akt (pAkt), on the other hand, was significantly increased ($p < 0.05$) in the urea-treated cells (0.98, 95%-CI[0.11, 0.82]), compared to the control group (0.32, 95%-CI[0.24, 0.40]), shown in figure 8. Consistently, beta actin was used as loading control.

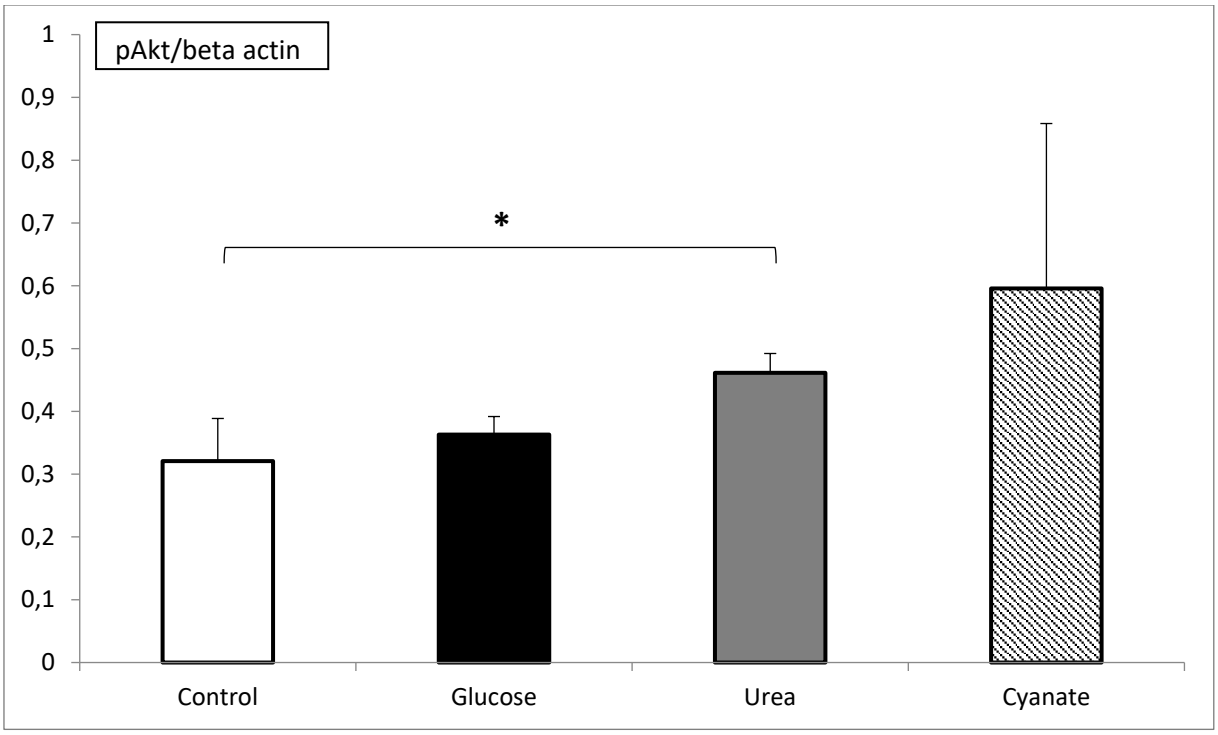

*Figure 8 | Increased pAkt expression in urea-treated h9c2 cells. Western blot analysis of h9c2 cells that were treated with glucose, urea, or cyanate for 30 minutes. pAkt expression was measured and compared to beta actin as a loading control. pAkt expression was significantly elevated in the urea-treated group. (Mean ± SD; n = 3 – 4 per group; * = p < 0.05 vs the control group; one-way ANOVA followed by Tukey's post-hoc test.)*

4.1.2 Upregulation of Akt and Erk in Urea/Oxalate model

In the heart samples of our animal model, we investigated changes of the factors Akt and Erk. We measured both the total amount and the phosphorylated protein via western blot and then analyzed the intensity with ImageJ. Figure 9 illustrates that the expression of Akt was significantly higher in the group that was fed urea and oxalate diet (2.31, 95%-CI[1.5, 3.12]) than in the control group (0.97, 95%-CI[0.73, 1.21]). The Erk expression, too, was significantly increased in the group that was fed urea and oxalate diet (0.76, 95%-CI[0.437, 1.08]) compared to the control group (0.2, 95%-CI[0.063, 0.337]). This experiment was conducted for 12 days.

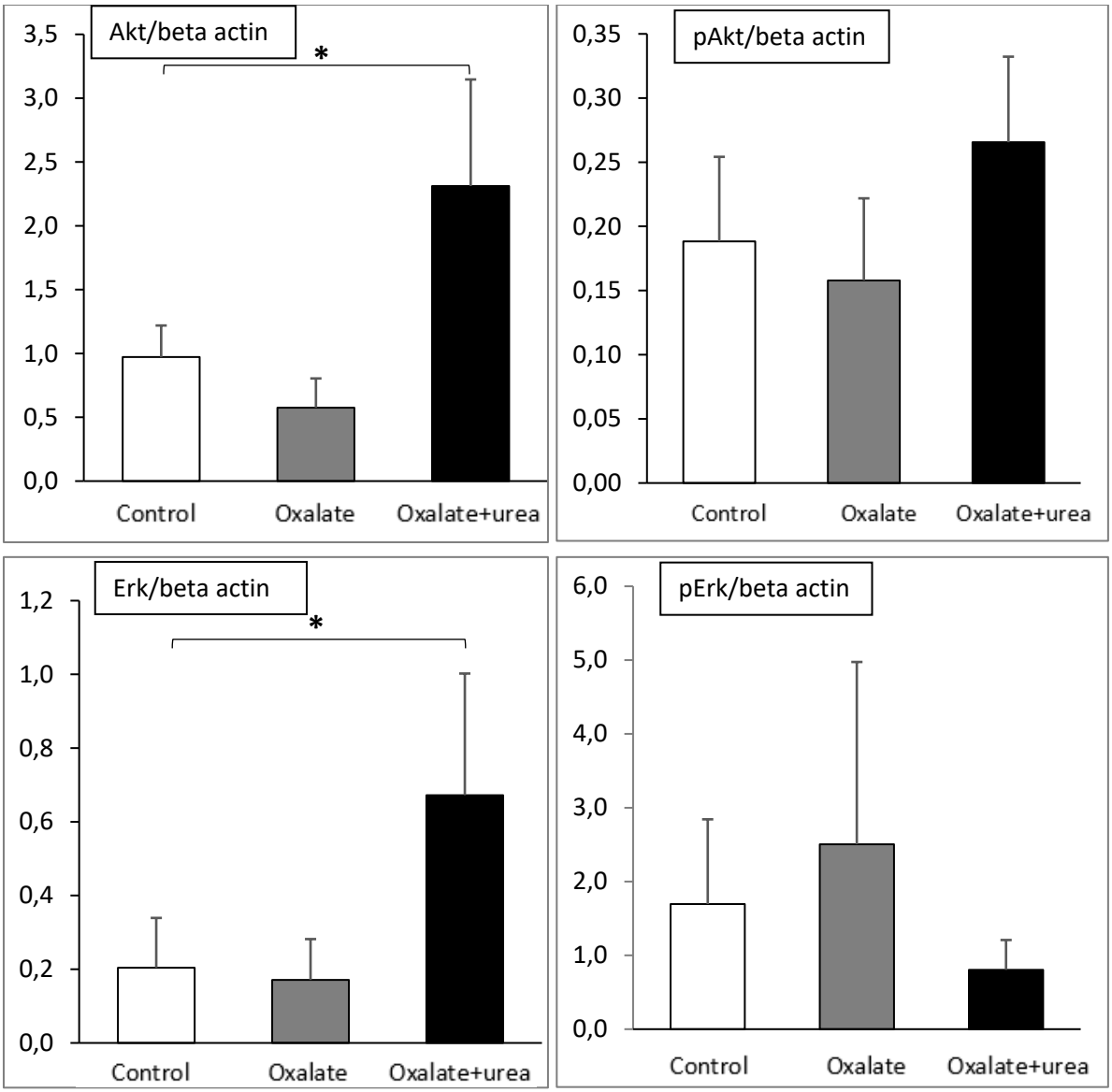

*Figure 9 | Western blot analysis of heart samples from mice that were given Oxalate or Urea + Oxalate diet for 12 days. Top left: Akt expression was significantly increased in the group that was fed with urea and oxalate. Akt expression was measured and compared to beta actin as loading control. Top right: Total amount of phosphorylated Akt was compared to beta actin. There was no significant difference. Bottom left: Erk expression was significantly increased in the group that was fed with urea and oxalate. Erk expression was measured and compared to beta actin as loading control. Bottom right: Total amount of phosphorylated Erk was compared to beta actin. There was no significant difference. (Mean ± SD; n = 4 per group; * = p < 0.05; one-way ANOVA followed by Tukey's post-hoc test.)*

4.2 Oxidative stress by urea treatment

To investigate oxidative stress in the urea-treated cells, we designed three different experiments: First, we analyzed the amino acids that are affected the most by oxidative stress. As second approach, we used fluorescent stains to visualize changes in superoxides and number of mitochondria. Third, we used Agilent Seahorse XF Mito Stress Test to analyze mitochondrial metabolism in the living cell.

4.2.1 Difference in reduced amino acids in the media of HL-1 cells

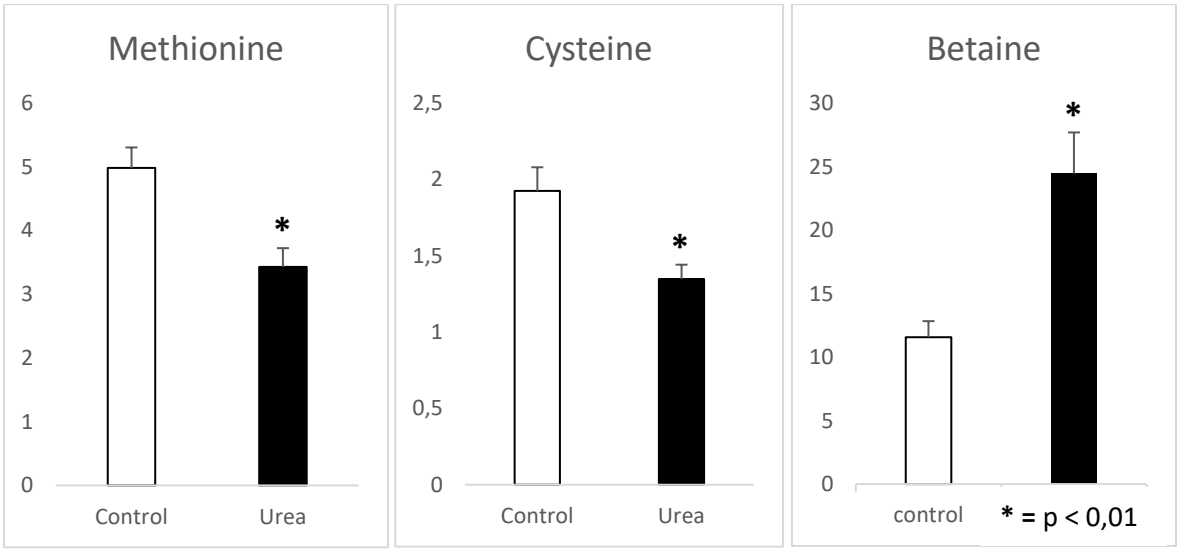

*Figure 10 | In the media of urea-treated HL-1 cells was a significant decrease of methionine and cysteine whereas betaine has been upregulated. HL-1 cells were treated with 40 mM Urea for 24 hours. We then analyzed the media via mass spectrometry. Left: Methionine was significantly decreased in the urea-treated group. Center: Cysteine was significantly decreased in the urea-treated group. Right: Betaine was significantly increased in the urea-treated group. (Mean ± SD; n = 3 per group; * = p < 0.01 vs the control group; Student t-test.)*

Figure 10 shows the results of a mass spectrometry analysis of free amino acids in the media of HL-1 cells. These cells were treated with urea for 24 hours. Illustrated are the results for the amino acids that, in our eyes, are the best indicators for oxidative processes: Methionine, cysteine and betaine. The amount of methionine (3.43, 99%-CI[2.89, 3.97]) was significantly reduced, compared to the control group (4.98, 99%-CI[4.40, 5.57]). Cysteine levels (1.35, 99%-

CI[1.32, 1.38]), too, were significantly decreased in comparison to the control group (1.93, 99%-CI[1.64, 2.21]), suggesting consumption by oxidative stress. Betaine (24.45, 99%-CI[19.65, 29.28]) levels were significantly elevated in the urea-treated group compared to the control group (11.57, 99%-CI[9.68, 13.40]).

4.2.2 No change of the number of mitochondria and concentration of ROS

We suspected that a change in metabolic function took place in long-time (>24 h) treated H9c2 cells. This change would affect the state of oxidative stress as well as mitochondrial function. We used Hoechst® nucleid acid stain to show integrity of the nucleus. MitoTracker Green FM (ThermoFisher) was used to stain mitochondria, and MitoSOX™ Red reagent (ThermoFisher) was used to determine the concentration of superoxides.

In figure 11 one picture is shown as an example for each of the four groups: 1. An untreated control; 2. Urea-treated cells (35mM urea); 3. Glucose-treated cells (25mM glucose); 4. Cyanate-treated cells (100µM).

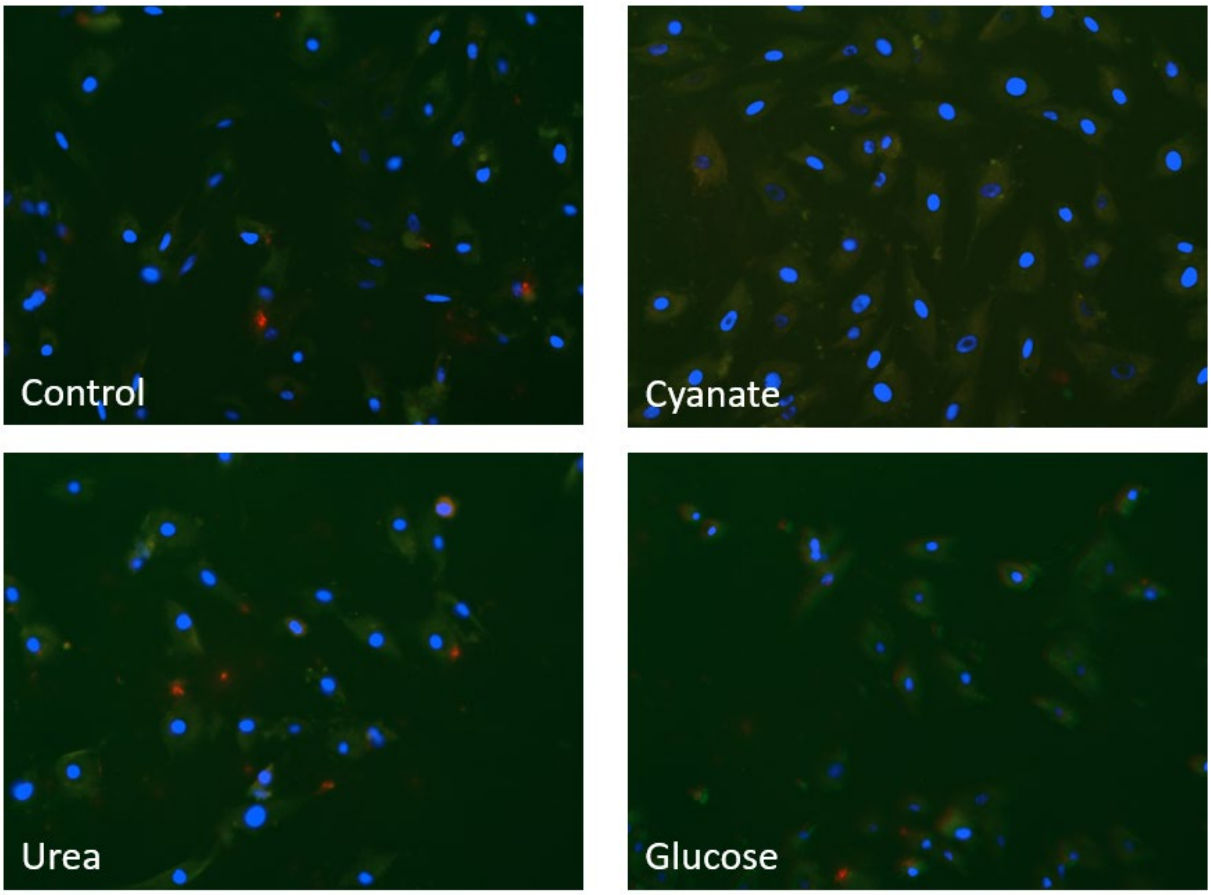

Figure 11 | Immunofluorescent staining for Cyanate, Urea, and Glucose. H9c2 cells were treated with 35 mM Urea, 25 mM glucose, or 100 mM cyanate for 48 hours. We used Mito-SOX™ Red reagent to detect ROS, MitoTracker Green FM to detect mitochondria, and Hoechst® nucleid acid to detect the nucleus. The staining reagents were left on the samples for 30 minutes. These are overlay pictures that show the three colors combined.

We measured the intensity of the different color stains via ImageJ® and blanked to the background noise. The different intensities were compared in three ways:

1. ROS to Mitochondria, to show oxidative stress in comparison to number of mitochondria
2. Mitochondria, to Nuclei, to investigate changes in the number of mitochondria
3. ROS to Nuclei, to show general oxidative stress.

The results are presented in figure 12 and show some differences in the urea-treated cells. In average, the level of oxidative stress and the number of mitochondria was higher in the urea-treated cells than in the other groups. But due to high deviation of background noise, we could not show any significance using this assay.

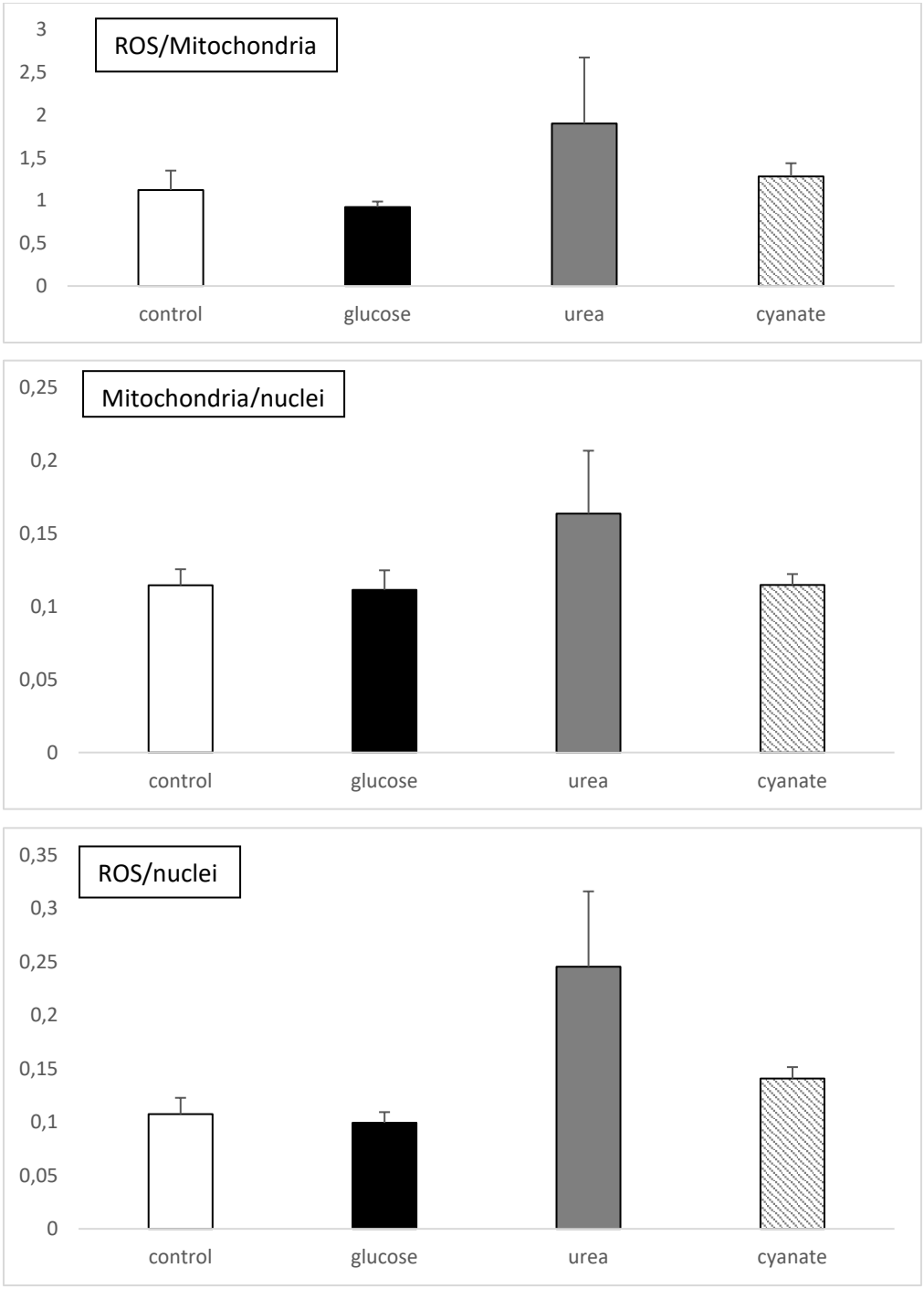

*Figure 12 | Intensity analysis for the colors red, green, and blue using ImageJ. For this analysis, we used the single-colored images, not the overlay. Top: Urea-treated cells showed a trend towards a higher amount of produced ROS adjusted for the number of mitochondria. There was no significance. (Mean ± SD; n = 6 per group, n = 10 for each image's fluorescence and n = 4 for each image's background; * = p < 0.05 vs the control group; one-way ANOVA followed by Tukey's post-hoc test.) Center: Urea-treated cells had more mitochondria than the other treatment groups. There was no significance. (Mean ± SD; n = 6 per group, n = 10 for each*

*image's fluorescence and n = 4 for each image's background; * = p < 0.05 vs the control group; one-way ANOVA followed by Tukey's post-hoc test.)* *Bottom: Urea-treated cells contained more ROS. (Mean ± SD; n = 6 per group, n = 10 for each image's fluorescence and n = 4 for each image's background; * = p < 0.05 vs the control group; one-way ANOVA followed by Tukey's post-hoc test.)*

4.3 H9c2 cells show significant difference in basal metabolism, uncoupling and reserve capacity

To measure key parameters of mitochondrial function, basal metabolism, uncoupling, and reserve capacity, we performed Agilent Seahorse XF Mito Stress Test. This assay made it possible to measure the oxygen consumption rate (OCR), basal respiration, proton leak, maximal respiration, spare respiratory capacity, and non-mitochondrial respiration. Figure 13 illustrates the succession of the experiment whereat an array indicates the adding of reagents that influence the cellular respiration.

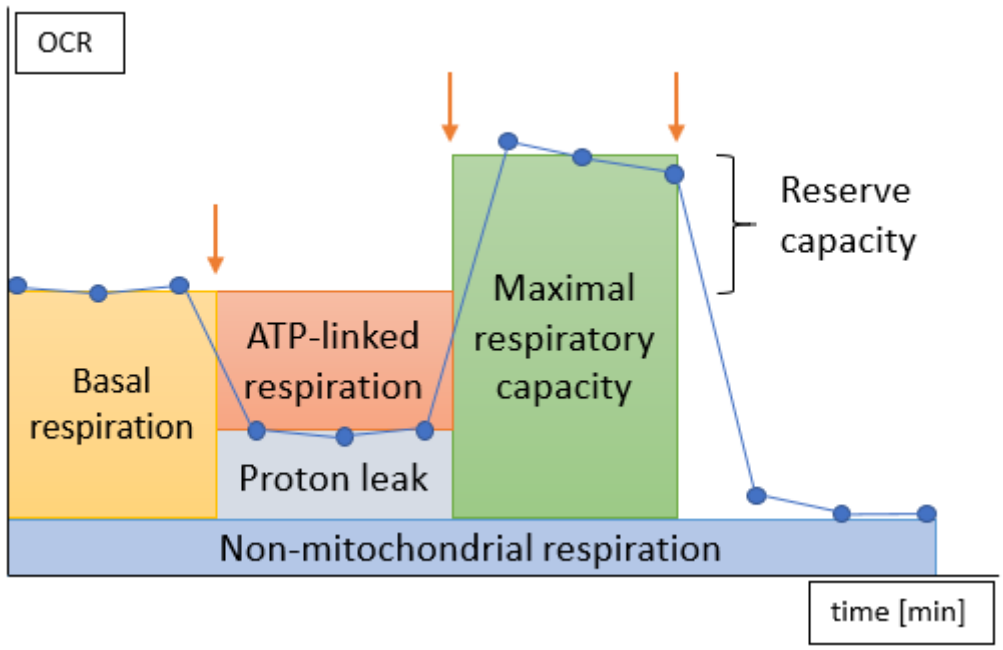

Figure 13 | Schematic diagram to illustrate Agilent Seahorse XF extracellular flux assay and mitochondrial function components. Modified from Agilent's website (www.agilent.com/en/products/cell-analysis-(seahorse)/mitochondrial-respiration-xf-cell-mito-stress-test). OCR was measured three times for each stage. The arrows indicate the addition of different regencies. 1. Oligomycin: Reversible inhibition of ATP-synthase/Complex V of the respiratory chain. This step subtracts the ATP-linked respiration from the basal respiration. 2. FCCP: Induction of uncoupling. This step induces the maximal respiration. 3. Rotenone/antimycin A: Inhibition of NADH dehydrogenase/Complex I of the respiratory chain. This step reveals non-mitochondrial respiration.

We performed Agilent Seahorse XF Mito Stress Test on h9c2 cells. The four groups were: Untreated cells, urea-treated cells (35mM), glucose-treated cells (25mM), and cyanate-

treated cells (35µM). Figure 14 shows the results of our experiment. It depicts twelve different time points which represent the following mitochondrial attributes (please also see figure 13 for graphic illustration):

Points 1-3 show the basal oxygen consumption rate (OCR), which compromises glycolysis and proton leak. At 20 min, oligomycin was added to reversely inhibit the ATP synthase (Complex V) to measure only glycolysis at points 4 – 6. The next three points (7 – 9) reveal maximal respiration, after the uncoupling agent FCCP was added at 40 min. At 60 min, we inhibited Complex I, so points 10 – 12 show only non-mitochondrial respiration. The shown data has been adjusted for amount of protein in each of the experiments' wells.

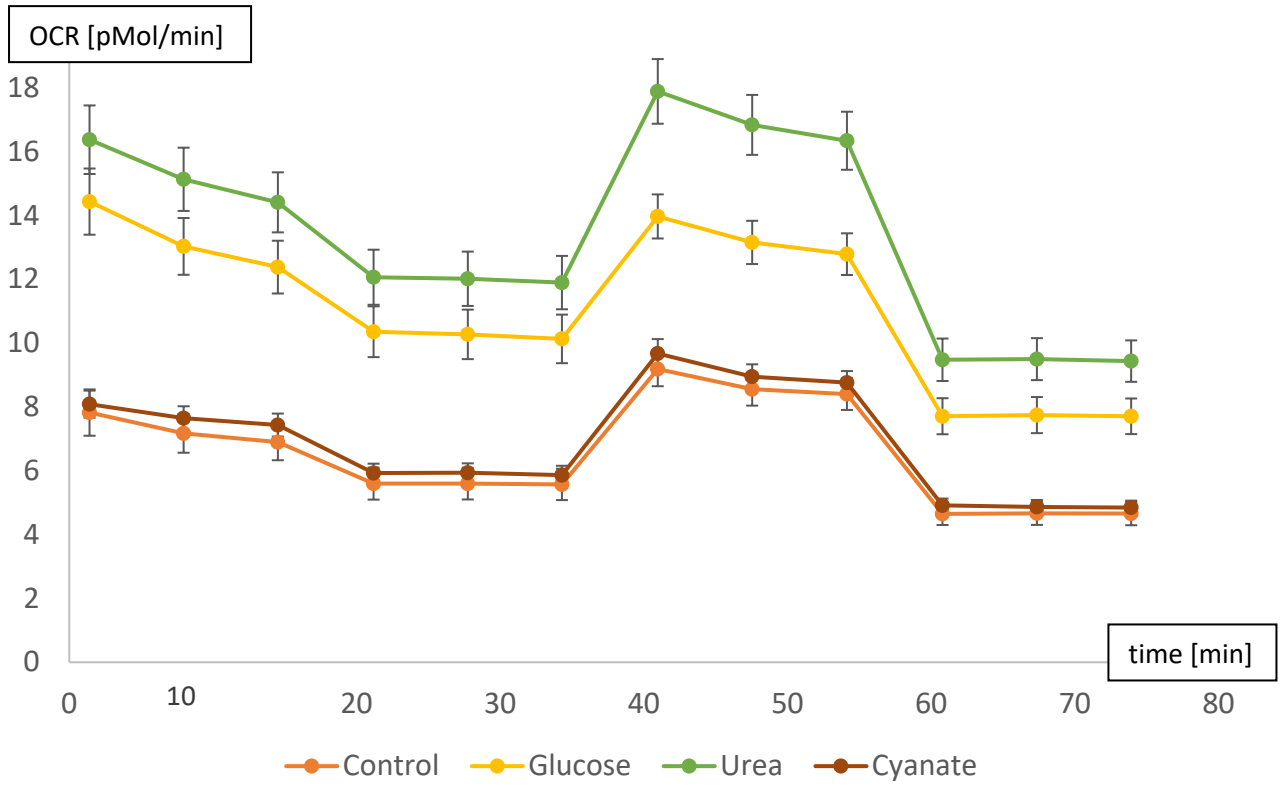

Figure 14 | Seahorse Mito Stress Test: Urea and glucose-treated cells had a higher OCR than cyanate-treated cells and the control group. OCR is shown vertically and time (in min) horizontally. H9c2-cells were treated with 35 mM urea, 25 mM glucose and 35 µM cyanate for 24 hours. Oligomycin was added at 20 min to inhibit ATP synthesis (complex V). FCCP was added at 40 min to disrupt the proton gradient and lead to maximal oxygen consumption. At 60 min, antimycin A and Rotenone were added to shut down mitochondrial metabolism. (Mean ± SD; n = 20 per group and timepoint, n = 4 for background noise per timepoint)

To have clearer results of mitochondrial respiration, we adjusted our data for non-mitochondrial respiration. This adjustment resulted in the following graph:

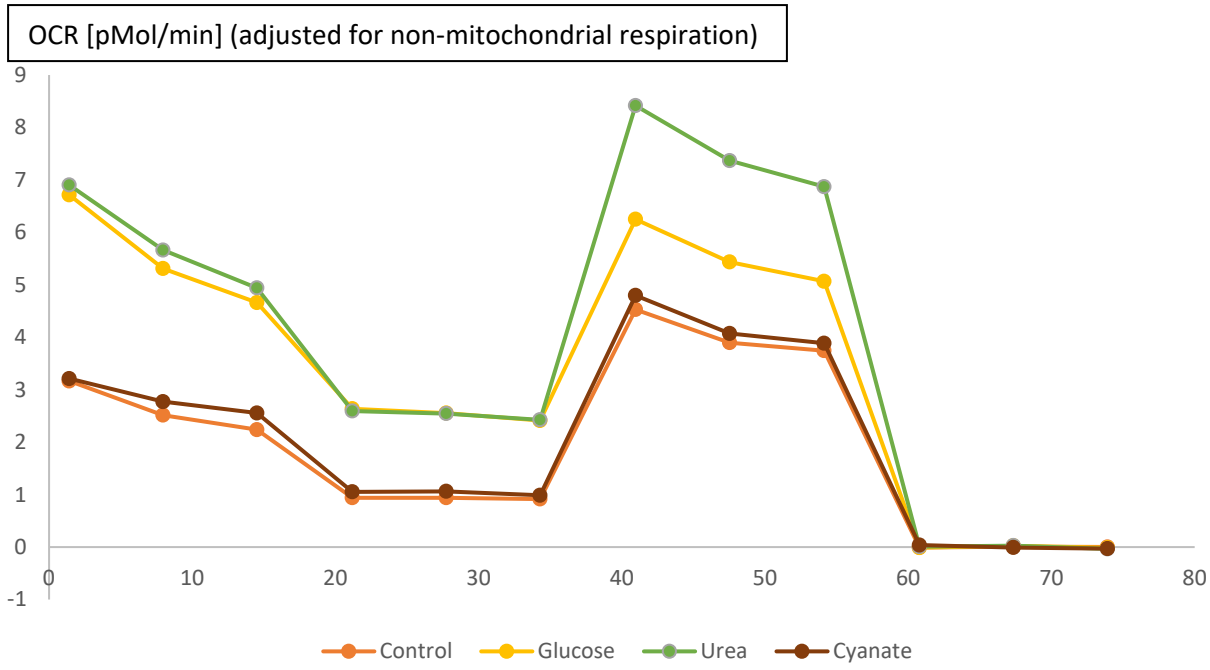

Figure 15 | Seahorse Mito Stress Test, adjusted for non-mitochondrial respiration: Urea and glucose-treated cells had a higher OCR than cyanate-treated cells and the control group. For timepoints 7 – 9, the urea-treated cells had a much steeper incline than the other groups. H9c2-cells were treated with 35 mM urea, 25 mM glucose and 35 µM cyanate for 24 hours. Oligomycin was added at 20 min to inhibit ATP synthesis (complex V). FCCP was added at 40 min to disrupt the proton gradient and lead to maximal oxygen consumption. (n = 20 per group and timepoint, n = 4 for background noise per timepoint)

Three findings emanated from the Seahorse XF experiment: Firstly, we found a significant difference ($p < 0.05$) in oxygen consumption rate (OCR) for the urea-treated cells (15.83, 95%-CI[13.52, 14.14]). Their OCR was higher than both, the cyanate-treated cells (14.14, 95%-CI[12.8, 15.5]) and the control group (12.54, 95%-CI[10.4, 14.6]), which indicates a higher rate of respiration. This data is shown in figure 16.

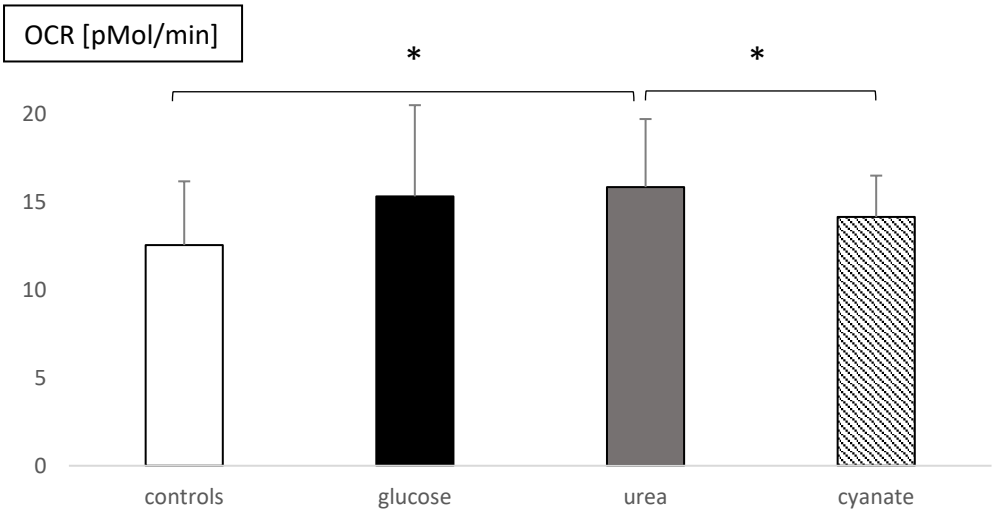

*Figure 16 | Oxygen consumption rate (OCR) was compared between the four investigated groups. The general OCR of the urea-treated cells was significantly higher than the control group ($p < 0.05$). Their OCR was even higher than the OCR of our positive control group, the cyanate-treated cells. Basal respiration (timepoints 1-3) was compared between the four groups of the Seahorse Mito Stress Test. (Mean ± SD; n = 20 per group and timepoint, n = 4 for background noise per timepoint; * = $p < 0.05$; one-way ANOVA followed by Tukey's post-hoc test.)*

Secondly, the oxygen consumption after inhibiting the ATP synthase, visualized at timepoints 4 – 6, was higher for the urea-treated cells (11.7, 99%-CI[10.1, 13.4]) and glucose-treated cells (11.19, 99%-CI[9, 13.4]) compared to the control group (9.16, 99%-CI[7.52, 10.8]) and represents the proton leak. The level of proton leak was about the same for glucose- and urea-treatment and was significantly elevated compared to the control group. Our positive control group, too, showed a significantly ($p < 0.05$) increased proton leak (10.55, 95%-CI[9.83, 11.3]) compared to the control group (9.16, 95%-CI[7.91, 10.4]).

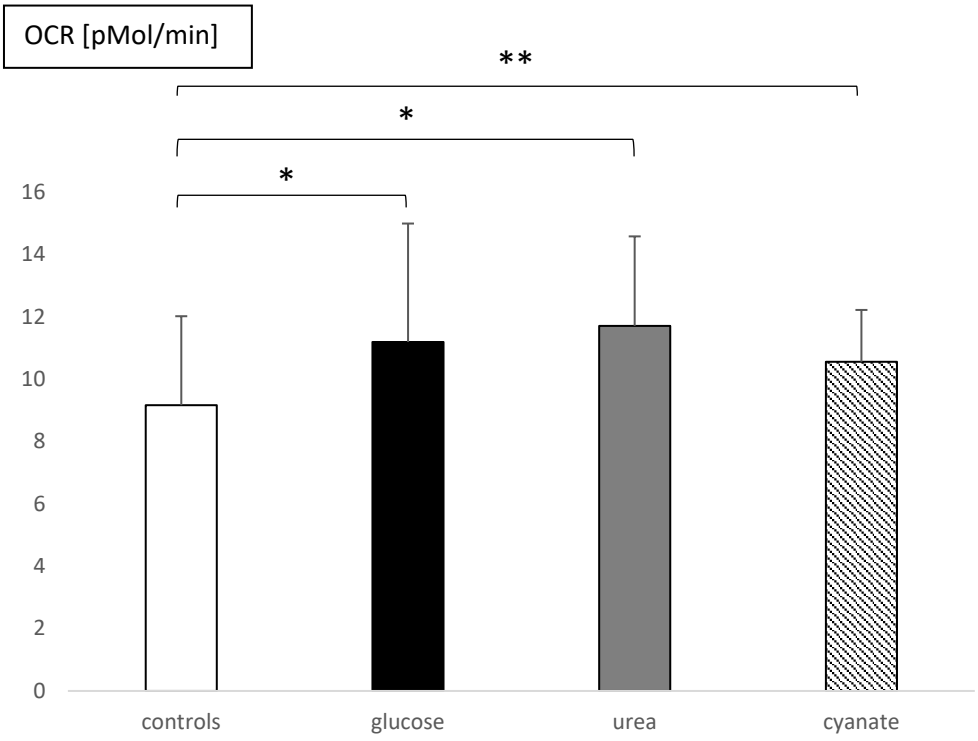

*Figure 17 | Proton leak was significantly higher for the glucose-, urea- and cyanate-treated group in the Seahorse Mito Stress Test. Oxygen consumption rate (OCR) was compared for the four investigated groups after inhibiting the ATP synthase (timepoints 4 – 6). The OCR of urea- (35 mM) and glucose-treated cells was about equally increased with high significance. The OCR of cyanate-treated cells was significantly increased. (Mean ± SD; n = 20 per group and timepoint, n = 4 for background noise per timepoint; * = p < 0.01 vs the control group, ** = p < 0.05 vs the control group; one-way ANOVA followed by Tukey's post-hoc test.)*

And lastly, our results showed a trend regarding the differences in maximal respiratory capacity. At timepoints 7 – 9, the urea-treated cells had the highest rate of oxygen consumption, after FCCP was added. At these timepoints, the glucose-treated cells had the second highest OCR. These results are illustrated in figure 18.

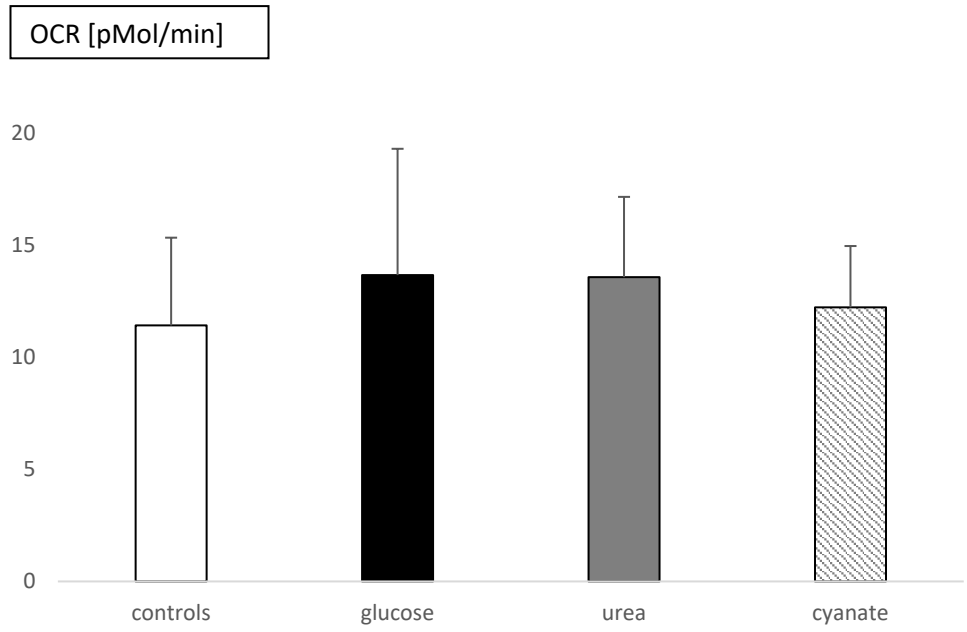

Figure 18 | Maximal respiratory capacity was higher in the urea -treated group in the Seahorse Mito Stress Test. Oxygen consumption rate (OCR) was compared for the four investigated groups after addition of FCCP (timepoints 7 – 9). (Mean ± SD; n = 20 per group and timepoint, n = 4 for background noise per timepoint; one-way ANOVA followed by Tukey's post-hoc test.)

5. DISCUSSION

In uremic cardiomyopathy, the major cardiac changes seen in patients are vascular and muscular impairments, such as micro-arteriopathy, fibrosis and left ventricular hypertrophy (LVH), the latter being its primary manifestation.(14, 16) It seems obvious that increased preload (hypervolemia) and afterload (elevated blood pressure, aortic stiffening) cause hypertrophic changes in the heart muscle, but experimental models of renal failure showed persistence of LVH despite correction of anemia and hypertension. More recent research concluded that the changes in ventricular function occur prior to measured structural changes.(42, 43) These findings suggest a different mechanism leading to the abovementioned pathophysiological changes in the heart.

5.1 Uremia and oxidative stress

Urea is produced mainly by liver and kidneys to prevent toxic levels of ammonium. Supraphysiological concentrations of urea are known to increase oxidative stress in cultured cells. D'Apolito, Du et al. found in 2010 that uremic mice, same as cultured cells, displayed insulin resistance and glucose intolerance. These effects could be normalized by treatment with an antioxidant SOD/catalase mimetic. In 2015 d'Apolito, comes to the conclusion that "urea itself, at levels common in patients with chronic renal failure, causes endothelial dysfunction and activation of proatherogenic pathways", which is conclusive with numerous research findings.(25, 26, 44-46) In our experiments, we used the urea concentration of 35 mM, which is the maximally accepted concentration in end-stage renal disease (ESRD).

In the search for the pathways linking uremia to cardiac failure, many investigators identified several dysregulations that lead to increased oxidative stress.(47) The induction of oxidative

stress has impaired cardiomyocyte viability in previous studies and reduction of oxidative stress has led to augmented survival of various cell types.(19, 20)

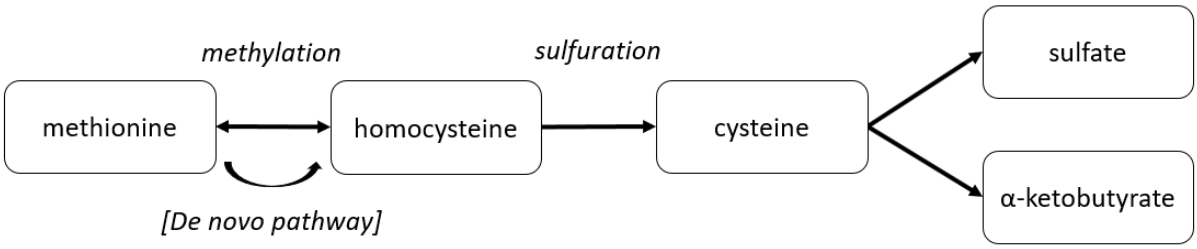

Figure 19 | The amino acids methionine, homocysteine and cysteine can be converted into each other via methylation and sulfuration. These amino acids are important for sustaining oxidative balance.

The amino acids methionine, homocysteine and cysteine are highly involved in sustaining the oxidative balance in the cell. Methionine, an essential amino acid, is necessary for protein synthesis and methylation.(48) For the latter, the "de novo pathway" is essential. Methionine is converted to S-adenosylmethionine (SAM), the principal methyl donor. SAM is needed in many cellular processes, such as cellular respiration, protein synthesis and proliferation, but it can also be converted to S-adenosylhomocysteine (SAH) and then hydrolyzed to homocysteine. Homocysteine may be converted to methionine via betaine-homocysteine S-methyltransferase (BHMT). In this reaction, betaine transfers a methyl group to homocysteine to become dimethylglycine. Other than its role as methyl donor, where BHMT is the only known enzyme that uses betaine as a substrate, betaine is a highly effective osmolyte that protects cells from environmental stress. Betaine has shown to protect internal organs and enhance performance of the heart.(49)

In summary, methionine and betaine are important cellular components to protect the cell from oxidative stress. In our experiments, we found a significant elevation of betaine in the media of the urea-treated cells. As betaine is consumed by regenerating methionine from homocysteine, the accumulation of betaine may indicate that the regeneration of methionine is diminished. Consistently, we could also measure a significantly decreased level of methionine. Methionine is an important antioxidant, as its sulfur atom is redox-active, so the significant decrease of methionine in the media would aggravate the oxidative state of a cell.(50)

Cysteine is a metabolite of methionine following the “trans-sulfuration pathway”. This pathway is the only irreversible elimination pathway for homocysteine, which then condenses with serine to form cystathionine. Cystathionine is split into cysteine, that is excreted with the urine, and α-ketobutyrate, that is oxidized in the Krebs cycle. Cysteine was significantly reduced after long-term treatment with urea. As trans-sulfuration depends on the methionine level, this finding is consistent with the low level of methionine described above. In conclusion, the low level of cysteine indicates that the trans-sulfuration pathway is not enhanced by urea treatment. Secondly, the reduction of cysteine is a marker for reactive oxygen species (ROS), as cysteine is necessary for the synthesis of glutathione, which is one of the most important non-enzymatic antioxidants that reduces ROS and thereby protects cells from oxidative stress. Therefore, a reduction of cysteine results in decreased synthesis of glutathione and thus increased oxidative stress.(51-53) Our findings regarding methionine, cysteine and betaine lead us to the conclusion that our cells are in a state of low antioxidative resources.

The trend towards higher oxidative stress was also measured in our fluorescent staining assay, where we found a higher amount of ROS as well as a higher number of mitochondria in the cells that underwent urea-treatment. Our results did not reach significance, but the tendency agrees with the findings of Li et al. that high uremic acid in concentrations of 15 mg/dl inhibits viability of h9c2 cardiomyocytes due to oxidative stress. They also determined the “ERK/p38 pathway” to connect uremia to the metabolic changes of cardiomyocytes.(19) This is also consistent with our findings regarding Erk being elevated in the urea-treated cells.

5.2 Urea’s pathway affecting cellular energy resilience

The extracellular signal regulated kinase 1 and 2 (Erk1/2, also called MAPK3/1) are closely related kinases that can phosphorylate myelin basic protein (MBP) and microtubule-associated protein-2 (MAP2). Therefore, they are of utmost importance in the transduction of extracellular signals, especially growth factor signaling.(54) Akt (PKB) is a serine/threonine kinase that plays a central role in promoting cell growth, proliferation and survival. It is part of a pathway that links extracellular signals via multiple receptor tyrosine kinases (mTOR and PI3K) to intracellular effectors. Because of these attributes, Akt is regarded as “a promising point of intervention for many cancers.”(55) But Akt also plays a key role in the control of

metabolic processes that lead to fibrosis, metabolic remodeling, vascular changes and hypertrophy.(56) These are the main symptoms of uremic cardiomyopathy. Our results of the urea/oxalate mouse model reveal a significant increase of both Akt and Erk. In this experiment, we also investigated the rate of phosphorylation of Akt and Erk. Probably, the rate of phosphorylation was not altered, as the experiment was conducted for 12 days and changes in phosphorylation usually occur in short-time treatments. Another explanation would be, that urea does not alter the phosphorylation of the investigated kinases but increases their rate of synthesis.

The fact that we could measure a similar increase in the urea-treated cells in the 24-hour treatment of h9c2 cells (Erk was significantly increased) indicates that this change is not only caused by the circulation of an organism adapting to kidney disease, but also by urea alone. This agrees with the finding of Winterberg et al. that "myocardial dysfunction occurs prior to changes in ventricular geometry in mice with chronic kidney disease (CKD)" and Li et al., who also found a reduced cardiomyocyte viability through the Erk-pathway.(19, 43) Also, it suggests the involvement of Akt and Erk in linking urea to intracellular changes leading to the symptoms of uremic cardiomyopathy. To connect these intracellular effectors to urea we propose the following pathway.

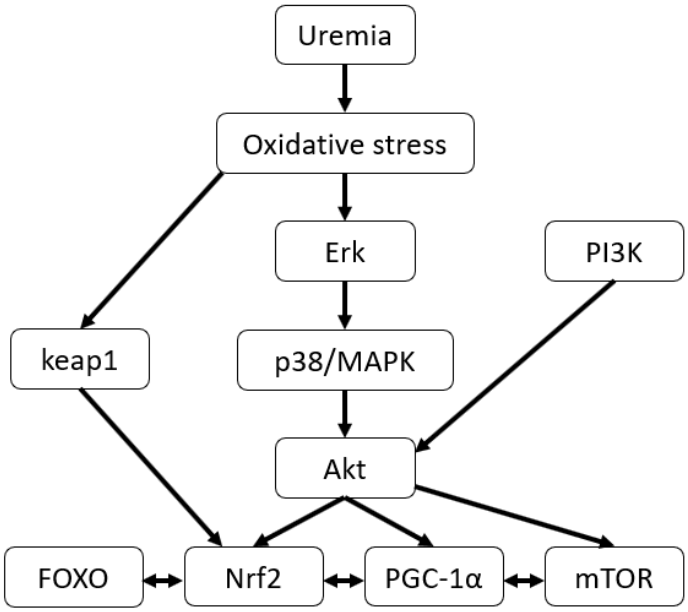

Figure 20 | The Erk/p38 pathway connects uremia, oxidative stress, and multiple upstream effectors to influence mitochondrial metabolism. Akt plays a central role, including PI3K signaling.

The Erk/p38 pathway has been discussed for its important regulatory impact on cell growth, metabolism, differentiation, and cell death. By the activation of this pathway, uremia causes impaired cardiomyocyte viability. Li et al. showed a time- and dose-dependent effect of urea on the viability of cardiomyocytes, consistent with other studies. They could also show a higher level of oxidative stress in their immunofluorescence assay, which is consistent with the trend towards oxidative stress that we found in our immunofluorescence staining assay of urea-treated cells.(19, 57)

P38 is one of the MAPKs (mitogen activated protein kinase), which are a family of serine/threonine kinases that control key cellular functions, such as proliferation and apoptosis. P38 is especially triggered by a range of cytotoxic stress and cytokines and moderates cell mortality. (57-59)

Keap1 (Kelch-like ECH-associated protein 1) and Nrf2 (Nuclear factor erythroid 2-related factor 2) are connected in a pathway that is the major regulator of cytoprotective responses to endogenous and exogenous stresses caused by reactive oxygen species (ROS) and electrophiles. Key signaling proteins are Nrf2, which binds to the antioxidant response element (ARE), and Keap1, a repressor protein of Nrf2 that promotes ubiquitination and degradation of Nrf2. Nrf2 is an important transcription factor encoding subunits from all five respiratory complexes. It is also involved in the transcription and replication of mitochondrial DNA. As it is of importance for the energy balance of the cell, the decreased activation of Nfr2 leads the cell to a state where it can no longer meet the requirements for an energetical resilient cardiomyocyte. (60, 61)

As patients with ESRD are more susceptible than the general population regarding cardiac and vascular mortality and this cardiac vulnerability has been linked to oxidative stress, the Keap1-Nrf2 pathway seems likely to play an important role in ESRD patients' mortality.(14, 47)

5.3 Uremia increases oxygen consumption

In uremic patients, cardiomyocytes need to be fit for the structural changes of the heart that lead to a progressive loss of cardiac contractility.(14, 62) Jefferies et al. confirmed in a study of patients with chronic kidney disease that their myocardium is more susceptible to ischemic damage. They also found that two thirds of adults and children receiving dialysis experience repeated episodes of intradialytic impairments in cardiac function.(63-65) These functional effects on the heart are part of the symptoms of uremic cardiomyopathy.

In our experiments we could show alterations in the metabolism of urea-treated h9c2 cells. The urea- and glucose-treated myocardial cells had a much higher oxygen consumption rate (OCR) than the untreated cells. The results did not reach significance for the glucose-treated cells. Their trend towards higher OCR may be explained by an increased metabolism caused by the provided supply of energy in form of glucose. Another factor is the elevated mitochondrial oxidative stress and inefficient metabolism due to uncoupling in hyperglycemic cells. Regarding the topic of diabetic cardiomyopathy (DCM), whose cellular alterations include fibrosis, insulin resistance and cardiac hypertrophy, many authors investigated the effect of hyperglycemia on cardiomyocytes. Findings from curated studies have connected cellular apoptosis in DCM to the increased generation of ROS.(66) Nishikawa et al. proved via inhibiting the electron transport chain that the increased generation of ROS in hyperglycemia is mainly caused by mitochondria.(67) Other studies confirmed this, as ROS scavenging could improve myocardial energetics in hyperglycemic rodents and in the h9c2 cell line.(66, 68) Therefore, our finding of elevated OCR in glucose-treated cells is conclusive with prior studies. As well as hyperglycemia, uremia has also been reported to increase levels of ROS in cell culture and in patients with end-stage renal disease.(25)

Insulin resistance is a common symptom and independent risk factor for vascular disease in patients with kidney disease. It has been thoroughly investigated in the field of Diabetic cardiomyopathy. Next to insulin resistance, there are also other factors leading to DCM. These factors include inflammation, transcriptional regulation and lipotoxins.(69) Nonetheless, insulin resistance and uremia might have a similar pathway causing cardiac hypertrophy. The connection between these two pathways seems to be the protein kinase AKT that is explained above and was discussed by Semple et al. in 2011.(56) Insulin resistance leads to increased ROS production in muscles. This is followed by an impaired mitochondrial oxidative capacity.

Conclusively, Bonnard et al. (2008) could show a reverse of insulin resistance in diet-induced diabetic mice by inhibition of mitochondrial ROS production.(70-72) In our experiment, we measured an increased oxygen consumption for the urea-treated cells. We adjusted the data for non-mitochondrial respiration, as we suspect an increasing mitochondrial energy wasting to be the main explanation, such as uncoupling or mitochondrial damage.

Physiologically, the mitochondrial respiratory complex pumps protons from the mitochondrial matrix to the intermembrane space to build up an electrochemical gradient, which is then used to generate ATP. A fraction of this potential is "uncoupled" from this process by uncoupling proteins and only generates heat, which for example is used for thermogenesis in brown adipose tissue.(73) Other explanations would be a damaged inner mitochondrial membrane, or electron slippage that would result in increased OCR without proton translocation.(74) Taylor et al. (2015) also reported that "mitochondrial respiration in the uremic heart is chronically uncoupled" in a rat model of chronic uremia. The authors suggest the mitochondrial permeability transition pore (mPTP) to play an important role regarding the mitochondrial uncoupling. This has been shown in a post-ischemia reperfusion model, where it might play a protective role by eliminating accumulated calcium from the matrix.(3, 75) Our finding of an elevated OCR leads us to the conclusion, that urea induces mitochondrial inefficiency, or even damages the myocardial cells. If the mPTP is affected by uremia, and not only by ischemia, is still to be investigated.

5.4 Urea-treated cells may have an increased reserve capacity

Interestingly, we found that the urea-treated cells probably have an increased reserve capacity, even though our results did not reach significance (see figure 18). In the measurement of OCR, we added FCCP to the living cells to induce maximal oxygen consumption. This enabled us to estimate the maximal potential respiration sustainable by the cells. A decrease of spare respiratory capacity indicates how close a cell is operating to its bioenergetic limit. After adding the uncoupling agent, oxygen consumption was highly elevated in the cells that underwent urea-treatment. This trend is best to be seen in figure 15 as the urea- and glucose-treated cells have a much steeper increase after FCCP is added.(74, 76) The increased reserve capacity could lead to the conclusion that urea, in some way, protects the cardiomyocyte regarding the

increasing energy demands in kidney failure. This protection was associated to increased Akt signaling by Wende et al. in 2015. Short-term activation of Akt was found to preserve cardiac function. Long-term activation, on the other hand, contributed to heart failure by inducing LVH and progressive repression of mitochondrial fatty acid oxidation pathways.(77) In our experiment, the cells were treated for 36 hours, which is a relatively short period of time to expect the induction of mitochondrial dysfunction.

5.5 PGC-1α and cardiac hypertrophy

PGC-1α is one of the transcription factors activated by Akt and is said to be the orchestrator of mitochondrial metabolism. Numerous signaling pathways transduce stimuli, such as stress, to the PGC-1α pathway. These pathways include MAPK, ß-adrenergic pathways, Ca^{2+}-dependent and NO-dependent pathways. PGC-1α, in turn, coactivates transcriptional partners, such as Nrf1 and -2, Tfam (Mitochondrial transcription factor A), FOXO (Forkhead box O), ERR (Estrogen related receptor) and, as its name indicates, PPARγ.(28, 61, 78-80)

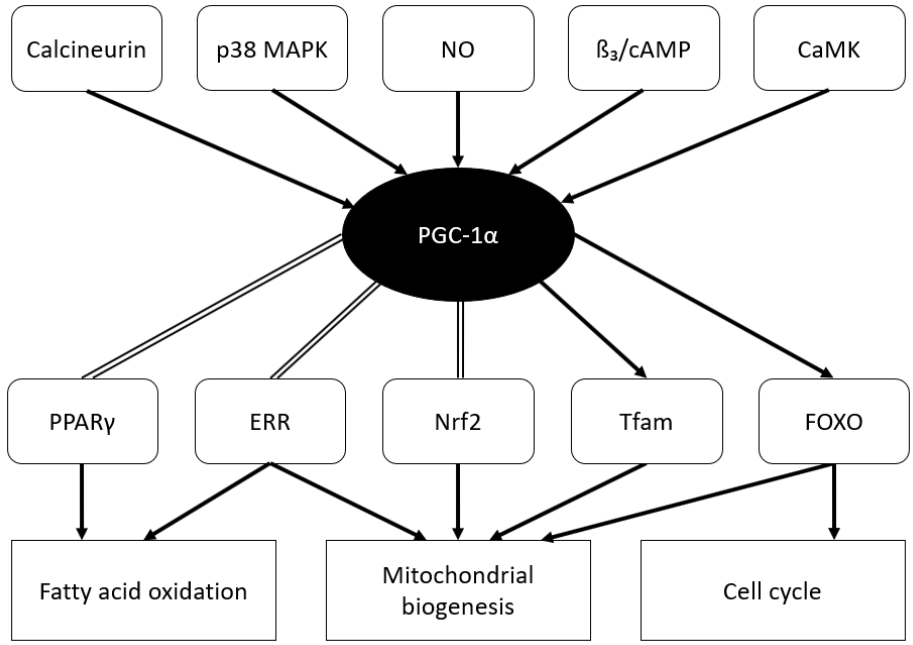

Figure 21 | PGC-1α integrates multiple pathways and regulates mitochondrial biogenesis, fatty acid oxidation and cell cycle. It is the master orchestrator of mitochondrial metabolism. The figure is an adaption to Huss and Kelly, 2005. Arrows indicate activation mediated by signal transduction pathways. Double lines indicate coactivation.(78)

The mitochondrial transcription factor A (Tfam or mtTFA) has been found to activate mitochondrial transcription and participate in mitochondrial genome replication. It encodes important proteins for the respiratory chain and is involved in mitochondrial fusion and fission.(80) Forkhead box O (FOXO) denotes a family of transcription factors that regulate the expression of different genes that affect cell survival and metabolism. FOXO, as well as Nrf2, is one of the binding partners of PGC-1α. In a model of Akt activation, PGC-1α was the most

repressed transcriptional gene, along with several binding partners such as Foxo1 and Nrf2. This reduction was found as early as 6 weeks in a mouse model of increased Akt activation.(77, 81) Our lab, previously, using primary cardiomyocytes, also showed that Urea decreases PGC-1α expression. In our animal model, four months of urea treatment decreased PGC-1α levels in the hearts of mice, too (data not shown). These findings add to the evidence that PGC-1α is an important mediator in uremic cardiomyopathy, therefore influencing ventricular hypertrophy.

Left ventricular hypertrophy (LVH) is the primary manifestation of uremic cardiomyopathy and said to predict mortality in patients with ESRD.(82) As explained above, LVH occurs not only as reaction to hypertension, but also in its absence. So, hypertrophy must have an intracellular precursor. We see urea as a uremic toxin that has been neglected for too long. Other authors discuss different uremic toxins. Examples of these substances are endothelin 1, parathyroid hormone, tumor necrosis factor α, leptin, interleukin 1α and interleukin 6.(83) The cardiotonic steroids Ouabain and Marinobufagenin are among these substances. These steroids act on the K-ATPase transmembrane protein on the surface of cardiomyocytes and lead to an increase of reactive oxygen species. As they can be filtered by a semipermeable membrane, they might present a good therapeutic target in the future.(16, 84)

Even though these toxins might influence the development of uremic cardiomyopathy, there has not been a clear finding that one of these substances alone leads to the cardiac changes seen in uremia. It seems more likely that many different toxins cause oxidative stress and alter the mitochondrial health of the cell. LVH in renal failure is characterized by cardiomyocyte hypertrophy and cardiomyocyte drop out. This can be caused by an impaired mitochondrial state of the cell. Regarding the explained pathways above, we see PGC-1α as a possibly important regulator of cardiac dysfunction and mitochondrial biogenesis in uremia.(45, 46)

6. CONCLUSION AND LIMITATIONS

6.1 Uremic cardiomyopathy – a puzzle with many pieces

The physiological and pathological influences on the oxidative system and mitochondrial function are numerous. PGC-1α is likely one of many players in uremic cardiomyopathy. Nonetheless, our results add to the scientific evidence of many authors that PGC-1α plays an important role, and that the Erk/p38 pathway is one of its main upstream effectors.

In 2009, Adhihetty et al. published a paper about a PGC-1α knockout mice. They found that the lack of PGC-1α lead to an alteration of mitochondrial composition and impaired mitochondrial respiratory function. Also, they looked at the state of oxidative stress and did not find the ROS to be affected. As we found increased oxidative stress in the urea-treated cells, it supports our conclusion that oxidative stress must be up-stream of PGC-1α (see figure 20).(85) Lack of PGC-1α was also found to impair the heart's ability to appropriately react to exercise and other stimuli that activate ß-adrenergic signaling. PGC-1α-KO-mice showed a decreased chronotropic response, although a decreased ventricular function could not be shown.(86) Other authors detected an upregulation of PGC-1α in response to ß-adrenergic stress and a lower cardiac energy state in response to uremia.(78, 87) As we did not research the physiological cardiac function in our mouse work, it is difficult to assess these findings. But it would be an interesting next step to look at the cardiac function of the uremic mice and see if there is a change in the chronotropic response to ß-adrenergic stress as well.

We found mitochondrial inefficiency to be the cause for the impaired efficiency of cardiomyocytes in uremia, but there is another possible explanation: Mitochondrial fusion and fission. It has become more and more evident in the last years that mitochondria are highly dynamic and undergo continuous changes that can be caused by oxidative stress, as well as by other factors of environmental stress (e.g. exercise, cold exposure and calorie restriction).(80, 88) In the heart, these processes are mainly caused be ischemia and reperfusion which then triggers two large guanosine triphosphatases (GTPases) to mediate fusion and fission processes. Damaged mitochondria are subjected to autophagy, which appears to be closely linked to the beforementioned processes. Therefore, mitochondrial inefficiency is likely not the sole reason

for impaired cardiomyocyte function, but it may be involved in the processes of mitochondrial biogenesis.(89, 90)

It should be considered that our cell culture and mouse model can only simulate the reality in the human body to a certain extent. We used different cardiomyocyte cell lines (HL-1, h9c2) and samples from our mouse model for our experiment. On the one hand, this gives us the opportunity to investigate our subject from different angles. On the other hand, one could say that we did not care enough for the replicability of our results and it is true that a much bigger quantity of repetitions of our experiments is necessary to come to binding conclusions. The extracellular flux analyzer is a well-established method to assess mitochondrial function in h9c2 cells. Even though the experiment worked very well for us, we would suggest searching the perfect seeding concentration for h9c2 cells prior to the analysis. Other authors suggest a number of 20-40K for the XF24 analyzer.(91, 92)

Even though our findings are consistent with many well-published papers, we only looked at a piece of the puzzle. The next steps of investigating uremic cardiomyopathy should be to strictly document the level of urea in patients' blood in a clinical trial and screen for cardiac events, as it is already done. This clinical study should include a group of participants whose level of urea is decreased more thoroughly than the control group, maybe by using peritoneal dialysis. After analyzing the resulting data, the findings could proof a toxic effect of so-called physiological concentrations of urea. Still, it remains difficult and unethical to measure levels of PGC-1α in the cardiomyocytes of human patients.

6.2 Clinical implications: Target cardioprotective pathways for ischemic resilience

In the field of ischemic tolerance of the heart, targeting cardioprotective pathways may present clinical strategies for patients with kidney disease. Dikow et al. discuss in their paper of 2012 possible findings in uremia: Intracellular signaling pathways for cell protection and ischemia are intact in a uremic state. Furthermore, the uremic cells seem to profit more from cardioprotective adaptations than cells that are not affected by the uremic milieu.(93) Byrne et al. (2012) even investigate the ischemic resilience of uremic cardiomyocytes that were pre- and post-conditioned in different states of ischemia in two different animal models. They found that the uremic myocardium reacts differently from myocardium not exposed to uremic toxins, as the uremic cells are much more susceptive to ischemic conditioning.(94) For renal patients with acute myocardial infarction the pathways that adapt in uremia, e.g. the Erk/p38 pathway discussed above, may be an interesting target.

6.3 Clinical implications: Carbamylated Albumin - a possible indicator of heart failure

Another limitation of our experiments is that we investigate possible pathways who influence the heart in uremia, but we do not have a way to detect the patients with renal disease who are the most at risk for a cardiac event. A continuous measurement of urea would be needed. Drechsler et al. discuss a different possibility: Carbamylated albumin (cAlb). Same as glycated albumin is used as indicator for the state of glycemia in a longer period of time, carbamylated albumin could be used for uremia.(95)

Carbamylation is a term used to describe the addition of a “carbamoyl” moiety (2CONH2) to a functional group. Chronically elevated urea promotes carbamylation of proteins and directly contributes to pro-atherogenic mechanisms. As Berg, Drechsler et al. explain in 2013 “urea is in equilibrium with cyanate (HNCO), a product of urea deamination whose central carbon is susceptible to nucleophilic attack from amines and thiols […] in vivo”. Protein carbamylation therefore is an unavoidable consequence of excess urea.(96) This urea-derived cyanate reaches concentrations of 140 nmol/L in patients with ESRD (45 nmol/L in healthy individuals) and leads to cellular responses, such as accelerated atherosclerosis and inflammation. Cyanate can produce irreversible modifications of primary amines and reversible modifications of

thiols, hydroxyls, phenols, and imidazole groups.(97) The effect of carbamylation was demonstrated by Kraus et al. by measuring exceeding concentrations of many carbamylated free amino acids in patients with ESRD, compared to their unmodified precursor.(98, 99) Carbamylation not only affects free amino acids. Like the glycation of hemoglobin, proteins are carbamylated, too, and recent studies reveal an association between elevated protein carbamylation and all-cause and cardiovascular mortality. As time-averaged urea concentrations and plasma protein carbamylation depict a strong correlation carbamylated Albumin could be used as a clinical parameter to predict cardiac risk. (96, 100, 101)

With cAlb as a predictor of cardiac threat, drugs can be developed for the patients who are at high risk with the aim to ameliorate their outcome. For this indication, many drugs are already being investigated. We hope that our research can help to find a better treatment for these patients.

7. SUMMARY

For the past 20 years, chronic kidney disease (CKD) has remained one of the major causes of death worldwide. Cardiovascular events account for approximately 50% of deaths in CKD patients, underscoring the clinical relevance of the observed cardiac changes. These changes define uremic cardiomyopathy (UCM) and include left-ventricular hypertrophy (LVH), LV dilatation, and LV systolic and diastolic dysfunction. LVH is seen as the primary manifestation of UCM and is caused by a multitude of different systems including increased pre- and afterload and the renin-angiotensin system (RAS). More recent studies found that myocardial dysfunction is apparent before changes in the ventricular geometry, like hypertrophy, occur to the uremic heart. This leads to the conclusion that LVH is not the cause of cardiac dysfunction, but one of the alterations caused by factors related to the uremic state itself. Among these factors that are independent of pressure and volume overload, are cardiotonic steroids as well as the parathyroid hormone and the endothelin (ET-1) system. But we suggest a different substance to play an important role in UCM: Urea. Patients in end-stage renal disease (ESRD) display increased oxidative stress and urea has been found to increase levels of oxidative stress, at least in endothelial cells. Therefore, we investigated the effect that elevated urea levels, as seen in patients undergoing dialysis, have on cardiomyocytes. As the oxidative stress in a cell is regulated by mitochondrial processes, we suspected the mitochondrial orchestrator PGC-1α to play an important role.

The uremic heart is in a state of elevated oxidative stress. This has been presented by multiple authors before. By conducting immunofluorescent staining for reactive oxygen species (ROS), we tried to replicate their findings and illustrate elevated levels of ROS. As the fluorescence analysis did not bear significant results, we approached oxidative stress from a different angle: Via mass spectrometry, we looked at the amino acids methionine, cysteine and betaine which are highly involved in sustaining the oxidative balance in the cell. Our findings in the media of urea-treated HL-1 cells lead us to the conclusion, that these cardiomyocytes were in a state of low antioxidative resources.

Next, to find the intracellular mechanisms that connect uremia to oxidative stress and compromised energetics, we investigated possible downstream effectors of uremia. The urea-treated cardiomyocytes exhibited significant alterations regarding upstream effectors of PGC-

1α: The protein kinases Akt and Erk were expressed and phosphorylated differently in a western blot analysis of uremic h9c2 cells and in mice with induced kidney failure. To combine these findings regarding the protein kinases Akt and Erk and oxidative stress, the Erk/p38 pathways seems conclusive (figure 20). This pathway links uremia and oxidative stress to intracellular effectors that have been found to influence the development of uremic cardiomyopathy.

Another life-threatening alteration in uremic cardiomyopathy is a corrupted cardiac function. The myocardium of uremic patients has shown to be more susceptible to ischemic damage and most patients receiving dialysis experience repeated episodes of intradialytic impairments in cardiac function. The urea-treated cardiomyocytes had a significantly higher oxygen consumption rate due to an inefficiently increased metabolism, most likely caused by an increased level of uncoupling.

Taken together, the results of this study indicate that urea by itself plays a role in the development of uremic cardiomyopathy. So-called high-physiologic levels of urea have led to a mitochondrial inefficiency and an increase of oxidative stress in cardiomyocytes. The protein kinases Akt and Erk may work as effectors of urea to induce these changes via the Erk/p38 pathway. It seems very likely that the mitochondrial changes are mediated by the mitochondrial orchestrator PGC-1α. These observations might lead to further studies investigating urea levels in dialysis patients. In the future, these might lead to a change of practice regarding tolerated urea levels in dialysis and help reduce the cardiac mortality of patients with chronic kidney disease.

8. ZUSAMMENFASSUNG

Chronische Niereninsuffizienz ist eine der häufigsten Todesursachen weltweit. Da etwa die Hälfte dieser Todesfälle auf kardiovaskuläre Ursachen zurückzuführen sind, ist ein genaues Verständnis der kardialen Veränderungen entscheidend. Zu diesen zählen linksventrikuläre Hypertrophie, linksventrikuläre Dilatation sowie systolischer und diastolischer Funktionsverlust. Zusammen prägen diese Veränderungen den Begriff der Urämischen Kardiomyopathie (UCM). Verschiedene Systeme spielen bei UCM zusammen, wie beispielsweise eine erhöhte Vor- und Nachlast und das Renin-Angiotensin-Aldosteron-System (RAAS). Sie führen zur primären Manifestation der UCM: Die linksventrikuläre Hypertrophie (LVH). Allerdings konnten aktuellere Studien zeigen, dass die Funktion des urämischen Myokards bereits abnimmt, noch bevor Veränderungen der Ventrikelstruktur, wie Hypertrophie, messbar sind. Demnach ist LVH nicht einzig die Ursache des kardialen Funktionsverlusts, sondern eine von vielen Veränderungen bei chronischer Niereninsuffizienz. Zu den Faktoren, die unabhängig von Blutdruck und Volumensteigerung sind und eine Rolle bei den oben geschilderten Veränderungen spielen, gehören kardiotonische Steroide, das Parathyroidhormon und das Endothelinsystem (ET-1-System). Wir sehen Grund zur Annahme, dass Urea (Harnstoff) ein weiterer dieser Faktoren ist, der zu Veränderungen des Herzmuskels führt und die Entstehung von UCM begünstigt. Dialysepatienten haben ein erhöhtes Level an oxidativem Stress und es wurde gezeigt, dass Urea in Endothelzellen zu erhöhtem oxidativem Stress führt. Deshalb behandelten wir Kardiomyozyten mit sogenannten hochphysiologischen Urea-Konzentrationen und untersuchten diese anschließend. Dabei setzten wir einen Schwerpunkt auf mitochondriale Prozesse, die zu erhöhtem oxidativen Stress führen können. Unser Interesse galt dabei insbesondere dem Transkriptionsfaktor PGC-1α, der als Regulator der Mitochondrien und Dirigent des intrazellulären Metabolismus gilt.

Um ebenfalls erhöhte Konzentrationen von oxidativem Stress nachzuweisen, experimentierten wir mit immunofluoreszenten Färbungen. Hierdurch konnten wir nur einen Trend ohne Signifikanz feststellen. Deshalb näherten wir uns dem Problem aus einer anderen Richtung: mittels Massenspektrometrie. Wir untersuchten die Aminosäuren Methionin, Cystein und Betain, die für die Regulation des oxidativen Gleichgewichts wichtig sind. Im Medium von mit Urea behandelten HL-1 Zellen konnten wir nachweisen, dass die untersuchten Kardiomyozyten signifikant geringere Konzentrationen an antioxidativ wirkenden Aminosäuren hatten.

Als nächstes untersuchten wir die intrazellulären Mechanismen zwischen Urämie und oxidativem Stress. In den mit Urea behandelten h9c2 Zellen und im Mausmodell fand sich eine signifikante Konzentrationssteigerung der Proteinkinase B (PKB/Akt) und Proteinkinase Erk. Diese Enzyme beeinflussen auch den Transkriptionsfaktor PGC-1α. Zusammenführen lassen sich unsere bisherigen Ergebnisse mittels der Erk/p38 Signalskaskade (Abb. 20). Urämie führt darin über Oxidativem Stress zu einer Beeinflussung intrazellulärer Effektoren, die zur Entstehung von Urämischer Kardiomyopathie beitragen.

Eine weitere lebensbedrohliche Komplikation von Urämischer Kardiomyopathie ist die Verringerung der Herzfunktion. Bei urämischen Patienten ist das Myokard anfälliger für ischämiebedingten Schaden und bei den meisten Dialysepatienten zeigen sich wiederholt Episoden, in denen die Herzfunktion geschwächt ist. In der Zellkultur konnten wir dazu passende Veränderungen nachweisen. Aufgrund eines ineffizienten Metabolismus verbrauchten die mit Urea behandelten Zellen signifikant mehr Sauerstoff. Ursache dafür ist wahrscheinlich ein vermehrtes Entkoppeln (Uncoupling) der Mitochondrien.

Zusammengefasst zeigt diese Studie, dass Urea in der Entwicklung von Urämischer Kardiomyopathie eine wichtige Rolle spielt. Hoch-physiologische Konzentrationen von Urea im Blut führen über die Erk/p38 Signalkaskade und die Proteinkinasen PKB und Erk zu einer ineffizienten Funktion der Mitochondrien und erhöhen den intrazellulären oxidativen Stress. Wir halten es für wahrscheinlich, dass der Transkriptionsfaktor PGC-1α die dazu führenden mitochondrialen Veränderungen reguliert. Diese Erkenntnisse können weitere Studien anregen, die die tolerierte Konzentration von Urea bei Dialysepatienten untersuchen. Zukünftig kann dies zu einer strengeren Einstellung der Urea-Werte bei Dialysepatienten führen. Möglicherweise lässt sich dadurch die Mortalität der Patienten mit chronischer Niereninsuffizienz senken.

9. LIST OF REFERENCES

1. Global, regional, and national life expectancy, all-cause mortality, and cause-specific mortality for 249 causes of death, 1980-2015: a systematic analysis for the Global Burden of Disease Study 2015. Lancet (London, England). 2016;388(10053):1459-544.
2. de Jager DJ, Grootendorst DC, Jager KJ, van Dijk PC, Tomas LM, Ansell D, et al. Cardiovascular and noncardiovascular mortality among patients starting dialysis. JAMA. 2009;302(16):1782-9.
3. Taylor D, Bhandari S, Seymour AM. Mitochondrial dysfunction in uremic cardiomyopathy. Am J Physiol Renal Physiol. 2015;308(6):F579-87.
4. Kasper. LF. Harrisons Innere Medizin.2012.
5. Andrassy KM. Comments on 'KDIGO 2012 Clinical Practice Guideline for the Evaluation and Management of Chronic Kidney Disease'. Kidney Int. 2013;84(3):622-3.
6. Kidney Disease: Improving Global Outcomes (KDIGO) CKD Work Group. KDIGO 2012 clinical practice guideline for the evaluation and management of chronic kidney disease. Kidney Int. 2013.
7. Davison SN, Levin A, Moss AH, Jha V, Brown EA, Brennan F, et al. Executive summary of the KDIGO Controversies Conference on Supportive Care in Chronic Kidney Disease: developing a roadmap to improving quality care. Kidney Int. 2015;88(3):447-59.
8. Bruck K, Stel VS, Gambaro G, Hallan S, Volzke H, Arnlov J, et al. CKD Prevalence Varies across the European General Population. Journal of the American Society of Nephrology : JASN. 2016;27(7):2135-47.
9. Collaboration GBDCKD. Global, regional, and national burden of chronic kidney disease, 1990-2017: a systematic analysis for the Global Burden of Disease Study 2017. Lancet (London, England). 2020;395(10225):709-33.
10. Webster AC, Nagler EV, Morton RL, Masson P. Chronic Kidney Disease. Lancet. 2017;389(10075):1238-52.
11. Frei US-H, H.J. Nierenersatztherapie in Deutschland. Bericht über Dialysebehandlungen und Nierentransplantationen in Deutschland. QuaSi-Niere.; 2007. Contract No.: ISBN 3-9809996-3-7.
12. Nolan CR. Strategies for improving long-term survival in patients with ESRD. Journal of the American Society of Nephrology : JASN. 2005;16 Suppl 2:S120-7.
13. Sarnak MJ, Levey AS, Schoolwerth AC, Coresh J, Culleton B, Hamm LL, et al. Kidney disease as a risk factor for development of cardiovascular disease: a statement from the American Heart Association Councils on Kidney in Cardiovascular Disease, High Blood Pressure Research, Clinical Cardiology, and Epidemiology and Prevention. Circulation. 2003;108(17):2154-69.
14. Wanner C, Amann K, Shoji T. The heart and vascular system in dialysis. Lancet. 2016;388(10041):276-84.
15. Chronic Kidney Disease Prognosis C, Matsushita K, van der Velde M, Astor BC, Woodward M, Levey AS, et al. Association of estimated glomerular filtration rate and albuminuria with all-cause and cardiovascular mortality in general population cohorts: a collaborative meta-analysis. Lancet. 2010;375(9731):2073-81.
16. Alhaj E, Alhaj N, Rahman I, Niazi TO, Berkowitz R, Klapholz M. Uremic cardiomyopathy: an underdiagnosed disease. Congest Heart Fail. 2013;19(4):E40-5.
17. Amann K, Wanner C, Ritz E. Cross-talk between the kidney and the cardiovascular system. Journal of the American Society of Nephrology : JASN. 2006;17(8):2112-9.
18. J. GORDON BETTS PD, EDDIE JOHNSON,JODY E. JOHNSON. Anatomy and Physiology. Houston, Texas 770052017.
19. Li Z, Shen Y, Chen Y, Zhang G, Cheng J, Wang W. High Uric Acid Inhibits Cardiomyocyte Viability Through the ERK/P38 Pathway via Oxidative Stress. Cell Physiol Biochem. 2018;45(3):1156-64.
20. Muzi-Filho H, Bezerra CG, Souza AM, Boldrini LC, Takiya CM, Oliveira FL, et al. Undernutrition affects cell survival, oxidative stress, Ca2+ handling and signaling pathways in vas deferens, crippling reproductive capacity. PLoS One. 2013;8(7):e69682.

21. Johnson WJ, Hagge WW, Wagoner RD, Dinapoli RP, Rosevear JW. Effects of urea loading in patients with far-advanced renal failure. Mayo Clinic proceedings. 1972;47(1):21-9.
22. Eknoyan G, Beck GJ, Cheung AK, Daugirdas JT, Greene T, Kusek JW, et al. Effect of dialysis dose and membrane flux in maintenance hemodialysis. N Engl J Med. 2002;347(25):2010-9.
23. Vaziri ND. Oxidative stress in uremia: nature, mechanisms, and potential consequences. Semin Nephrol. 2004;24(5):469-73.
24. Zhang Z, Dmitrieva NI, Park JH, Levine RL, Burg MB. High urea and NaCl carbonylate proteins in renal cells in culture and in vivo, and high urea causes 8-oxoguanine lesions in their DNA. Proceedings of the National Academy of Sciences of the United States of America. 2004;101(25):9491-6.
25. D'Apolito M, Du X, Zong H, Catucci A, Maiuri L, Trivisano T, et al. Urea-induced ROS generation causes insulin resistance in mice with chronic renal failure. The Journal of clinical investigation. 2010;120(1):203-13.
26. D'Apolito M, Du X, Pisanelli D, Pettoello-Mantovani M, Campanozzi A, Giacco F, et al. Urea-induced ROS cause endothelial dysfunction in chronic renal failure. Atherosclerosis. 2015;239(2):393-400.
27. Wu Z, Puigserver P, Andersson U, Zhang C, Adelmant G, Mootha V, et al. Mechanisms controlling mitochondrial biogenesis and respiration through the thermogenic coactivator PGC-1. Cell. 1999;98(1):115-24.
28. Patten IS, Arany Z. PGC-1 coactivators in the cardiovascular system. Trends Endocrinol Metab. 2012;23(2):90-7.
29. Puigserver P, Wu Z, Park CW, Graves R, Wright M, Spiegelman BM. A cold-inducible coactivator of nuclear receptors linked to adaptive thermogenesis. Cell. 1998;92(6):829-39.
30. Uguccioni G, Hood DA. The importance of PGC-1alpha in contractile activity-induced mitochondrial adaptations. Am J Physiol Endocrinol Metab. 2011;300(2):E361-71.
31. Goto M, Terada S, Kato M, Katoh M, Yokozeki T, Tabata I, et al. cDNA Cloning and mRNA analysis of PGC-1 in epitrochlearis muscle in swimming-exercised rats. Biochem Biophys Res Commun. 2000;274(2):350-4.
32. Rowe GC, Jiang A, Arany Z. PGC-1 coactivators in cardiac development and disease. Circ Res. 2010;107(7):825-38.
33. Handschin C, Spiegelman BM. Peroxisome proliferator-activated receptor gamma coactivator 1 coactivators, energy homeostasis, and metabolism. Endocr Rev. 2006;27(7):728-35.
34. Garnier A, Fortin D, Delomenie C, Momken I, Veksler V, Ventura-Clapier R. Depressed mitochondrial transcription factors and oxidative capacity in rat failing cardiac and skeletal muscles. J Physiol. 2003;551(Pt 2):491-501.
35. Arany Z, He H, Lin J, Hoyer K, Handschin C, Toka O, et al. Transcriptional coactivator PGC-1 alpha controls the energy state and contractile function of cardiac muscle. Cell Metab. 2005;1(4):259-71.
36. Lehman JJ, Barger PM, Kovacs A, Saffitz JE, Medeiros DM, Kelly DP. Peroxisome proliferator-activated receptor gamma coactivator-1 promotes cardiac mitochondrial biogenesis. J Clin Invest. 2000;106(7):847-56.
37. Vega RB, Huss JM, Kelly DP. The coactivator PGC-1 cooperates with peroxisome proliferator-activated receptor alpha in transcriptional control of nuclear genes encoding mitochondrial fatty acid oxidation enzymes. Mol Cell Biol. 2000;20(5):1868-76.
38. Lin J, Wu H, Tarr PT, Zhang CY, Wu Z, Boss O, et al. Transcriptional co-activator PGC-1 alpha drives the formation of slow-twitch muscle fibres. Nature. 2002;418(6899):797-801.
39. Lin Y, Berg AH, Iyengar P, Lam TK, Giacca A, Combs TP, et al. The hyperglycemia-induced inflammatory response in adipocytes: the role of reactive oxygen species. J Biol Chem. 2005;280(6):4617-26.
40. Mulay SR, Eberhard JN, Pfann V, Marschner JA, Darisipudi MN, Daniel C, et al. Oxalate-induced chronic kidney disease with its uremic and cardiovascular complications in C57BL/6 mice. Am J Physiol Renal Physiol. 2016:ajprenal 00488 2015.

41. Mulay SR, Eberhard JN, Pfann V, Marschner JA, Darisipudi MN, Daniel C, et al. Oxalate-induced chronic kidney disease with its uremic and cardiovascular complications in C57BL/6 mice. Am J Physiol Renal Physiol. 2016;310(8):F785-F95.
42. Rambausek M, Ritz E, Mall G, Mehls O, Katus H. Myocardial hypertrophy in rats with renal insufficiency. Kidney Int. 1985;28(5):775-82.
43. Winterberg PD, Jiang R, Maxwell JT, Wang B, Wagner MB. Myocardial dysfunction occurs prior to changes in ventricular geometry in mice with chronic kidney disease (CKD). Physiol Rep. 2016;4(5).
44. Ritz E, McClellan WM. Overview: increased cardiovascular risk in patients with minor renal dysfunction: an emerging issue with far-reaching consequences. J Am Soc Nephrol. 2004;15(3):513-6.
45. McMahon AC, Greenwald SE, Dodd SM, Hurst MJ, Raine AE. Prolonged calcium transients and myocardial remodelling in early experimental uraemia. Nephrol Dial Transplant. 2002;17(5):759-64.
46. Amann K, Tyralla K, Gross ML, Schwarz U, Tornig J, Haas CS, et al. Cardiomyocyte loss in experimental renal failure: prevention by ramipril. Kidney Int. 2003;63(5):1708-13.
47. Rubattu S, Mennuni S, Testa M, Mennuni M, Pierelli G, Pagliaro B, et al. Pathogenesis of chronic cardiorenal syndrome: is there a role for oxidative stress? Int J Mol Sci. 2013;14(11):23011-32.
48. Finkelstein JD. Methionine metabolism in mammals. J Nutr Biochem. 1990;1(5):228-37.
49. Craig SA. Betaine in human nutrition. Am J Clin Nutr. 2004;80(3):539-49.
50. Torres M, Forman HJ. Redox signaling and the MAP kinase pathways. Biofactors. 2003;17(1-4):287-96.
51. Cavuoto P, Fenech MF. A review of methionine dependency and the role of methionine restriction in cancer growth control and life-span extension. Cancer Treat Rev. 2012;38(6):726-36.
52. Alirezaei M, Khoshdel Z, Dezfoulian O, Rashidipour M, Taghadosi V. Beneficial antioxidant properties of betaine against oxidative stress mediated by levodopa/benserazide in the brain of rats. J Physiol Sci. 2015;65(3):243-52.
53. van Guldener C, Stam F, Stehouwer CD. Hyperhomocysteinaemia in chronic kidney disease: focus on transmethylation. Clin Chem Lab Med. 2005;43(10):1026-31.
54. Boulton TG, Cobb MH. Identification of multiple extracellular signal-regulated kinases (ERKs) with antipeptide antibodies. Cell Regul. 1991;2(5):357-71.
55. Freeman-Cook KD, Autry C, Borzillo G, Gordon D, Barbacci-Tobin E, Bernardo V, et al. Design of selective, ATP-competitive inhibitors of Akt. J Med Chem. 2010;53(12):4615-22.
56. Semple D, Smith K, Bhandari S, Seymour AM. Uremic cardiomyopathy and insulin resistance: a critical role for akt? Journal of the American Society of Nephrology : JASN. 2011;22(2):207-15.
57. Wang X, Liu JZ, Hu JX, Wu H, Li YL, Chen HL, et al. ROS-activated p38 MAPK/ERK-Akt cascade plays a central role in palmitic acid-stimulated hepatocyte proliferation. Free Radic Biol Med. 2011;51(2):539-51.
58. Jha SK, Jha NK, Kar R, Ambasta RK, Kumar P. p38 MAPK and PI3K/AKT Signalling Cascades inParkinson's Disease. Int J Mol Cell Med. 2015;4(2):67-86.
59. Morrison RS, Kinoshita Y, Johnson MD, Ghatan S, Ho JT, Garden G. Neuronal survival and cell death signaling pathways. Adv Exp Med Biol. 2002;513:41-86.
60. Kansanen E, Kuosmanen SM, Leinonen H, Levonen AL. The Keap1-Nrf2 pathway: Mechanisms of activation and dysregulation in cancer. Redox Biol. 2013;1:45-9.
61. Scarpulla RC. Transcriptional activators and coactivators in the nuclear control of mitochondrial function in mammalian cells. Gene. 2002;286(1):81-9.
62. Amann K, Breitbach M, Ritz E, Mall G. Myocyte/capillary mismatch in the heart of uremic patients. J Am Soc Nephrol. 1998;9(6):1018-22.
63. Ix JH, Shlipak MG, Liu HH, Schiller NB, Whooley MA. Association between renal insufficiency and inducible ischemia in patients with coronary artery disease: the heart and soul study. J Am Soc Nephrol. 2003;14(12):3233-8.

64. Wetmore JB, Broce M, Malas A, Almehmi A. Painless myocardial ischemia is associated with mortality in patients with chronic kidney disease. Nephron Clin Pract. 2012;122(1-2):9-16.
65. Jefferies HJ, Virk B, Schiller B, Moran J, McIntyre CW. Frequent hemodialysis schedules are associated with reduced levels of dialysis-induced cardiac injury (myocardial stunning). Clin J Am Soc Nephrol. 2011;6(6):1326-32.
66. Arkat S, Umbarkar P, Singh S, Sitasawad SL. Mitochondrial Peroxiredoxin-3 protects against hyperglycemia induced myocardial damage in Diabetic cardiomyopathy. Free Radic Biol Med. 2016;97:489-500.
67. Nishikawa T, Edelstein D, Du XL, Yamagishi S, Matsumura T, Kaneda Y, et al. Normalizing mitochondrial superoxide production blocks three pathways of hyperglycaemic damage. Nature. 2000;404(6779):787-90.
68. Ilkun O, Wilde N, Tuinei J, Pires KM, Zhu Y, Bugger H, et al. Antioxidant treatment normalizes mitochondrial energetics and myocardial insulin sensitivity independently of changes in systemic metabolic homeostasis in a mouse model of the metabolic syndrome. J Mol Cell Cardiol. 2015;85:104-16.
69. Nakamura M, Sadoshima J. Cardiomyopathy in obesity, insulin resistance and diabetes. J Physiol. 2020;598(14):2977-93.
70. Levelt E, Gulsin G, Neubauer S, McCann GP. MECHANISMS IN ENDOCRINOLOGY: Diabetic cardiomyopathy: pathophysiology and potential metabolic interventions state of the art review. Eur J Endocrinol. 2018;178(4):R127-R39.
71. Bonnard C, Durand A, Peyrol S, Chanseaume E, Chauvin MA, Morio B, et al. Mitochondrial dysfunction results from oxidative stress in the skeletal muscle of diet-induced insulin-resistant mice. J Clin Invest. 2008;118(2):789-800.
72. Hoehn KL, Salmon AB, Hohnen-Behrens C, Turner N, Hoy AJ, Maghzal GJ, et al. Insulin resistance is a cellular antioxidant defense mechanism. Proc Natl Acad Sci U S A. 2009;106(42):17787-92.
73. Berardi MJ, Shih WM, Harrison SC, Chou JJ. Mitochondrial uncoupling protein 2 structure determined by NMR molecular fragment searching. Nature. 2011;476(7358):109-13.
74. Butler MG, Hossain WA, Tessman R, Krishnamurthy PC. Preliminary observations of mitochondrial dysfunction in Prader-Willi syndrome. Am J Med Genet A. 2018.
75. Korge P, Yang L, Yang JH, Wang Y, Qu Z, Weiss JN. Protective role of transient pore openings in calcium handling by cardiac mitochondria. J Biol Chem. 2011;286(40):34851-7.
76. Brand MD, Nicholls DG. Assessing mitochondrial dysfunction in cells. Biochem J. 2011;435(2):297-312.
77. Wende AR, O'Neill BT, Bugger H, Riehle C, Tuinei J, Buchanan J, et al. Enhanced cardiac Akt/protein kinase B signaling contributes to pathological cardiac hypertrophy in part by impairing mitochondrial function via transcriptional repression of mitochondrion-targeted nuclear genes. Mol Cell Biol. 2015;35(5):831-46.
78. Huss JM, Kelly DP. Mitochondrial energy metabolism in heart failure: a question of balance. J Clin Invest. 2005;115(3):547-55.
79. Czubryt MP, McAnally J, Fishman GI, Olson EN. Regulation of peroxisome proliferator-activated receptor gamma coactivator 1 alpha (PGC-1 alpha) and mitochondrial function by MEF2 and HDAC5. Proc Natl Acad Sci U S A. 2003;100(4):1711-6.
80. Ventura-Clapier R, Garnier A, Veksler V. Transcriptional control of mitochondrial biogenesis: the central role of PGC-1alpha. Cardiovasc Res. 2008;79(2):208-17.
81. Eijkelenboom A, Burgering BM. FOXOs: signalling integrators for homeostasis maintenance. Nat Rev Mol Cell Biol. 2013;14(2):83-97.
82. de Bie MK, van Dam B, Gaasbeek A, van Buren M, van Erven L, Bax JJ, et al. The current status of interventions aiming at reducing sudden cardiac death in dialysis patients. Eur Heart J. 2009;30(13):1559-64.
83. Winchester JF, Audia PF. Extracorporeal strategies for the removal of middle molecules. Semin Dial. 2006;19(2):110-4.

84. Kennedy DJ, Vetteth S, Periyasamy SM, Kanj M, Fedorova L, Khouri S, et al. Central role for the cardiotonic steroid marinobufagenin in the pathogenesis of experimental uremic cardiomyopathy. Hypertension. 2006;47(3):488-95.
85. Adhihetty PJ, Uguccioni G, Leick L, Hidalgo J, Pilegaard H, Hood DA. The role of PGC-1alpha on mitochondrial function and apoptotic susceptibility in muscle. Am J Physiol Cell Physiol. 2009;297(1):C217-25.
86. Leone TC, Lehman JJ, Finck BN, Schaeffer PJ, Wende AR, Boudina S, et al. PGC-1alpha deficiency causes multi-system energy metabolic derangements: muscle dysfunction, abnormal weight control and hepatic steatosis. PLoS Biol. 2005;3(4):e101.
87. Chesser AM, Harwood SM, Raftery MJ, Yaqoob MM. Myocardial bioenergetic abnormalities in experimental uremia. Int J Nephrol Renovasc Dis. 2016;9:129-37.
88. Lin HY, Lai RH, Lin ST, Lin RC, Wang MJ, Lin CC, et al. Suppressor of cytokine signaling 6 (SOCS6) promotes mitochondrial fission via regulating DRP1 translocation. Cell Death Differ. 2013;20(1):139-53.
89. Youle RJ, van der Bliek AM. Mitochondrial fission, fusion, and stress. Science. 2012;337(6098):1062-5.
90. Li Y, Liu X. Novel insights into the role of mitochondrial fusion and fission in cardiomyocyte apoptosis induced by ischemia/reperfusion. J Cell Physiol. 2018;233(8):5589-97.
91. Ali Pour P, Kenney MC, Kheradvar A. Bioenergetics Consequences of Mitochondrial Transplantation in Cardiomyocytes. J Am Heart Assoc. 2020;9(7):e014501.
92. Chen X, Li X, Zhang W, He J, Xu B, Lei B, et al. Activation of AMPK inhibits inflammatory response during hypoxia and reoxygenation through modulating JNK-mediated NF-kappaB pathway. Metabolism: clinical and experimental. 2018;83:256-70.
93. Dikow R, Hardt SE. The uremic myocardium and ischemic tolerance: a world of difference. Circulation. 2012;125(10):1215-6.
94. Byrne CJ, McCafferty K, Kieswich J, Harwood S, Andrikopoulos P, Raftery M, et al. Ischemic conditioning protects the uremic heart in a rodent model of myocardial infarction. Circulation. 2012;125(10):1256-65.
95. Drechsler C, Kalim S, Wenger JB, Suntharalingam P, Hod T, Thadhani RI, et al. Protein carbamylation is associated with heart failure and mortality in diabetic patients with end-stage renal disease. Kidney Int. 2015;87(6):1201-8.
96. Berg AH, Drechsler C, Wenger J, Buccafusca R, Hod T, Kalim S, et al. Carbamylation of serum albumin as a risk factor for mortality in patients with kidney failure. Sci Transl Med. 2013;5(175):175ra29.
97. Stark GR. Reactions of cyanate with functional groups of proteins. 3. Reactions with amino and carboxyl groups. Biochemistry. 1965;4(6):1030-6.
98. Nilsson L, Lundquist P, Kagedal B, Larsson R. Plasma cyanate concentrations in chronic renal failure. Clin Chem. 1996;42(3):482-3.
99. Kraus LM, Jones MR, Kraus AP, Jr. Essential carbamoyl-amino acids formed in vivo in patients with end-stage renal disease managed by continuous ambulatory peritoneal dialysis: isolation, identification, and quantitation. J Lab Clin Med. 1998;131(5):425-31.
100. Kalim S, Karumanchi SA, Thadhani RI, Berg AH. Protein carbamylation in kidney disease: pathogenesis and clinical implications. Am J Kidney Dis. 2014;64(5):793-803.
101. Tang WH, Shrestha K, Wang Z, Borowski AG, Troughton RW, Klein AL, et al. Protein carbamylation in chronic systolic heart failure: relationship with renal impairment and adverse long-term outcomes. J Card Fail. 2013;19(4):219-24.

10. APPENDIX

10.1 ABBREVIATIONS

µM	Micromole
µm	Micrometer
^{o}C	Degrees Celsius
Ab	Antibody
ACN	Acetonitrile
ACR	Albumin to creatinine ratio
AER	Albumin excretion rate
Ag	Antigen
Akt	Protein kinase B
ANOVA	Analysis of variance
APS	Ammonium persulfate
ARE	Antioxidant response element
ATP	Adenosine triphosphate
BHMT	Betaine-homocysteine S-methyltransferase
bME	Beta-mercaptoethanol
cAlb	Carbamylated albumin
cAMP	Cyclic adenosine monophosphate
cDNA	Complementary DNA
CGA	Cause, glomerular filtration rate, and albuminuria
CKD	Chronic kidney disease
DALY	Disability-adjusted life-year
DAPI	4,6-diamino-2-phenylindole, dihydrochloride
DCM	Diabetic cardiomyopathy
ddH_2O	Double distilled water
DEPC	Diethyl pyrocarbonate
DMEM	Dulbecco's Modified Eagle's Medium
DMSO	Dimethyl Sulfoxide
DNA	Deoxyribonucleic acid
ECAR	Extracellular acidification rate
EDTA	Ethylenediaminetetraacetic acid
EGF	Epidermal growth factor
ERA	European Renal Association
Erk	Extracellular signal-regulated kinase
ERR	Estrogen related receptor
ESRD	End-stage renal disease
ET	Endothelin
FBS	Fetal bovine serum
FCCP	Carbonyl cyanide-4-(trifluoromethoxy)phenylhydrazone
FGF	Fibroblast grow factor
FOXO3a	Forkhead-Box-Protein O3A
GFR	Glomerular filtration rate
GTP	Guanosine triphosphate
h	Hour

HBSS	Hanks' Balanced Salt Solution
HEK	Human Embryonic Kidney Cells
HNCO	Cyanate
HPLC	High-performance liquid chromatography
IACUC	Institutional Animal Care and Use Committee
IGF	Insulin-like growth factor
JNK	C-Jun N-terminal kinase
KDIGO	Kidney Disease: Improving Global Outcomes
Keap1	Kelch-like ECH-associated protein 1
KO	Knock-out
kV	Kilovolt
LC-MS/MS	Liquid chromatography–mass spectrometry
LVH	Left-ventricular hypertrophy
M	Mole
mA	Milliampere
MAPK	Mitogen activated protein kinase
min	Minute
ml	Milliliter
mM	Minimole
mm	Millimeter
MOPS	3-(N-morpholino)propanesulfonic acid
mPTP	Mitochondrial permeability transition pore
mRNA	Messenger RNA
ms	Millisecond
mTOR	Mammalian target of rapamycin
nM	Nanomole
NO	Nitric oxide
Nrf2	Nuclear factor erythroid 2-related factor 2
OCR	Oxygen consumption rate
p38	p38 mitogen-activated protein kinase
PAGE	Polyacrylamide gel electrophoresis
pAKT	Phosphorylated Akt
PBS	Phosphate buffered saline
PCR	Polymerase chain reaction
pErk	Phosphorylated Erk
PGC-1α	Peroxisome proliferator-activated receptor-γ (PPARγ) coactivator-1α
PGC-1β	Peroxisome proliferator-activated receptor-γ (PPARγ) coactivator-1β
PI3K	Phosphoinositide 3-kinase
PMSF	Phenylmethylsulfonyl fluoride
PPARγ	Peroxisome proliferator-activated receptor-γ
PTH	Parathyroid hormone
PVDF	Polyvinylidene fluoride
RAAS	Renin-angiotensin-aldosterone system
RIPA	Radioimmunoprecipitation assay
RNA	Ribonucleic acid
ROS	Reactive oxygen species
rpm	Revolutions per minute
SAH	S-adenosylhomocysteine

SAM	S-adenosylmethionine
SDS	Sodium dodecyl sulfate
TBS	Tris-buffered saline
TCA cycle	Tricarboxylic acid cycle; Krebs cycle
TEMED	Tetramethylethylenediamine
Tfam	Mitochondrial transcription factor A
UCM	Uremic cardiomyopathy
UCP	Uncoupling protein; Thermogenin
VEGF	Vascular endothelial growth factor
WT	Wild type

10.2 ACKNOWLEDGEMENTS

An erster Stelle gilt Dank meinem Doktorvater Herrn Prof. Dr. med. Christoph Wanner für die gute Betreuung und die große Unterstützung bei der Planung der Promotion. Seine Offenheit für einen Forschungsaufenthalt in Boston sowie die Kooperation mit Prof. Anders Berg, MD, PhD, machten die Promotion zu einer spannenden und durchwegs positiven Erfahrung. Für sein Vertrauen und für seine persönliche Förderung bin ich sehr dankbar.

Frau PD Dr. med. Christiane Drechsler danke ich herzlich für die hervorragende Betreuung und das Mentoring vor allem gegen Ende der experimentellen Tätigkeiten sowie für die stets konstruktive Kritik beim Verschriftlichen dieser Arbeit.

Ganz besonderer Dank gilt Prof. Anders Berg, MD, PhD, für die Aufnahme in seinem Labor am Beth Israel Deaconess Medical Center in Boston. Ihm danke ich für seine gute Lehre und für seine kritische und motivierende Herangehensweise an wissenschaftliche Fragestellungen. Meiner Kollegin Dr. Mahtab Tavasoli, PhD, danke ich für die stets freundliche und kompetente Unterstützung. Sie vermittelte mir neben zahlreichen Methoden auch die Begeisterung an der Wissenschaft.

Dank aussprechen möchte ich auch der Deutschen Herzstiftung e.V., für die Förderung durch das „Kaltenbach Doktorandenstipendium“. Dem Würzburger Nierenverein e.V. danke ich für die Unterstützung durch das Reisestipendium, und der Medizinischen Fakultät und der Graduate School of Life Sciences (GSLS) der Universität Würzburg danke ich für die Förderung durch das Promotionsstipendium.

Von ganzem Herzen danken möchte ich letztlich meiner Familie, insbesondere meinen Eltern Anja und Jürgen Bergmann. Sie haben mich in meinem gesamten bisherigen Werdegang stets unterstützt, ermutigt, mitgefiebert und mir die Möglichkeit gegeben meine Ziele zu erreichen.

Zuletzt möchte ich mich bei meinen Freundinnen und Freunden bedanken. Danke für die wertvollen Gespräche, das Korrekturlesen dieser Arbeit und für die vielen unvergesslichen Momente der letzten Jahre.

Danke!

10.3 CURRICULUM VITAE

Tim J. Bergmann

SCHOLARSHIPS

Promotionsstipendium of the Graduate School of Life Sciences Würzburg, January 2017

Kaltenbach Doktorandenstipendium of the Deutschen Herzstiftung e.V., October 2016

Travel Scholarship of the Würzburger Nierenverein, August 2016

Scholarship from the Studienstiftung des deutschen Volkes, January 2014

Scholarship for an excellent High School diploma from e-fellows, June 2012

Würzburg, 11/11/2020

10.4 PUBLICATIONS AND PRESENTATIONS

10.4.1 PUBLICATION

"NCoR1-independent mechanism plays a role in the action of the unliganded thyroid hormone receptor"

Arturo Mendoza, Inna Astapova, Hiroaki Shimizu, Molly Gallop, Lujain Al-Sowaimel, Dileas MacGowan, **Tim Bergmann**, Anders H Berg, Danielle E. Tenen, Christopher Jacobs, Anna Lyubetskaya, Linus Tsai, Anthony N. Hollenberg.
Proceedings of the National Academy of Sciences 114(40):201706917

10.4.2 POSTER PRESENTATION

"Taurine Protects Against Urea-Induced Protein Carbamylation and Renal Fibrosis in an Oxalate Model of Kidney Injury"

Mahtab Tavasoli, S Ananth Karumanchi, Zsuzsanna K. Zsengeller, Isaac E. Stillman, **Tim Bergmann**, Sahir Kalim and Anders H. Berg.
Kidney Week, American Society of Nephrology, San Diego USA, October 2018

10.5 AFFIDAVIT/ EIDESSTATTLICHE ERKLÄRUNG

I hereby confirm that my thesis entitled “Pathways in uremic cardiomyopathy – the intracellular orchestrator PGC-1α in cell culture and in a mouse model of uremia“ is the result of my own work. I did not receive any help or support from commercial consultants. All sources and/or materials applied are listed and specified in the thesis.

Furthermore, I confirm that this thesis has not yet been submitted as part of another examination process neither in identical nor in similar form.

Hiermit erkläre ich an Eides statt, die Dissertation „Intrazelluläre Vorgänge bei Urämischer Kardiomyopathie – die Rolle von PGC-1α in Zellkultur und im Mausmodell“ eigenständig, d.h. insbesondere selbständig und ohne Hilfe eines kommerziellen Promotionsberaters, angefertigt und keine anderen als die von mir angegebenen Quellen und Hilfsmittel verwendet zu haben.

Ich erkläre außerdem, dass die Dissertation weder in gleicher noch in ähnlicher Form bereits in einem anderen Prüfungsverfahren vorgelegen hat.

Würzburg, 11/11/2020